CPT-BASED AXIAL CAPACITY DESIGN METHOD FOR DRIVEN PILES IN CLAY

by

Barry M. Lehane[1], Zhongqiang Liu[2], Eduardo J. Bittar[3] , Farrokh Nadim[4], Suzanne Lacasse[5], Nezam Bozorgzadeh[6], Richard Jardine[7], Jean-Christophe Ballard[8], Pasquale Carotenuto[9], Kenneth Gavin[10], Robert B. Gilbert[11], Jens Bergan-Haavik[12], Philippe Jeanjean F. ASCE[13] and Neil Morgan[14]

[1]Corresponding author, Professor, School of Engineering, The University of Western Australia, 6009, Australia. Email: *Barry.Lehane@uwa.edu.au*

[2]Senior Engineer, Norwegian Geotechnical Institute, P.O. Box. 3930 Ullevål Stadion, N-0806 Oslo, Norway. Email *Zhongqiang.Liu@ngi.no*

[3]PhD student, School of Engineering, The University of Western Australia, 6009, Australia. Email: *eduardo.bittarmarin@research.uwa.edu.au*

[4]Technical Director, Norwegian Geotechnical Institute, P.O. Box. 3930 Ullevål Stadion, N-0806 Oslo, Norway. Email *Farrokh.Nadim@ngi.no*

[5]Expert Advisor, Norwegian Geotechnical Institute, P.O. Box. 3930 Ullevål Stadion, N-0806 Oslo, Norway. Email *Suzanne.Lacasse@ngi.no*

[6]Professor, Dept. of Civil and Environmental Engineering, Imperial College, London SW7 2BU, UK. Email *r.jardine@imperial.ac.uk*

[7]Academic visitor, Norwegian Geotechnical Institute, P.O. Box. 3930 Ullevål Stadion, N-0806 Oslo, Norway. Email *Nezam.bozorgzadeh@ngi.no*

[8]Principal Engineer, Fugro Belgium, Rue du Bosquet, 1348 Louvain-la-Neuve, Belgium, Email *jc.ballard@fugro.com*

[9]Senior Engineer, Norwegian Geotechnical Institute, P.O. Box. 3930 Ullevål Stadion, N-0806 Oslo, Norway. Email *Pasquale.Carotenuto@ngi.no*

[10]Professor, Faculty of Civil Engineering and Geosciences Building, Delft University of Technology, 23 Stevinweg 1, PO box 5048 2628, Delft, The Netherlands. Email: *k.g.gavin@tudelft.nl*

[11]Professor, Department of Civil, Architectural and Environmental Engineering, The University of Texas at Austin, TX 78712. Email: *bob_gilbert@mail.utexas.edu*

[12]Principal Engineer, DNV AS, Veritasveien 1, 1363 Høvik, Norway. Email *jens.bergan.haavik@dnv.com*

[13]Senior Advisor, BP America, 501 Westlake Park Boulevard, Houston, TX 77079. Email:*Philippe.Jeanjean@bp.com*

[14]Principal Engineer, Lloyd's Register EMEA, Aberdeen AB15 8PJ, UK. Email *Neil.Morgan@lr.org*

Abstract

There are clear advantages in the establishment of reliable, direct CPT-based methods for assessment of the axial capacity of driven piles. These advantages motivated the formation of a Joint Industry Project (JIP) under the management of the Norwegian Geotechnical Institute (NGI), which initially led to the creation of a "Unified" database of high-quality pile load tests in sand and clay. The Unified database has the general consensus of representatives in the profession and personnel in multiple companies from the offshore energy sector. This paper presents a component of the research from the second phase of the JIP, which had the objective of developing a new CPT-based method for driven piles in clay to "unify" several CPT-based methods that are in use today. A rational basis for the CPT-based formulation is first described, using trends from instrumented pile tests, that facilitates an understanding of the approach and illustrates its empirical nature and limitations. The Unified database is used to calibrate the formulation and this is subsequently shown to lead to good predictions for an independent database of pile load tests and for measured distributions of shaft friction.

Introduction

Estimates of the axial capacity of driven piles in clay depend primarily on the assessment of shaft friction (τ_f), which typically represents a major proportion of the axial capacity. The alpha (α) design method proposed by API (2011) is currently the most common approach used to assess τ_f and assumes that τ_f varies directly with the triaxial compression unconsolidated undrained (UU) shear strength of the clay (s_u^{UU}) via an α factor (or 'adhesion' factor). The α value is expressed as an empirical function of the undrained strength ratio (s_u^{UU}/σ'_{v0}) which has been determined from a best-fit to capacities measured in a database of pile load tests (Randolph & Murphy 1985). Application of α approaches usually requires drilling and sampling boreholes and subsequent undrained strength tests on a representative number of nominally undisturbed samples. The cost of such an investigation coupled with the discrete nature of sampling and the well-known variability in s_u data due to sampling disturbance and other effects prompted the investigation into a new cone penetration test (CPT) based method presented in this paper.

Relationships between shaft friction and the CPT measured and corrected cone end resistances (q_c and q_t) for driven piles in clay have been proposed for many years e.g. Bustamante & Gianeselli (1982), Almeida et al. (1996), Lehane et al. (2000, 2013), Eslami & Fellenius (1997) and Niazi & Mayne (2016). This paper builds upon this earlier research and presents a new CPT-based method that is calibrated using a new database of pile load tests that was compiled by a team of experts working for a large Joint Industry Project (JIP) (Lehane et al. 2017). The sand and the clay pile test databases compiled for this JIP are referred to as "Unified" databases as they comprise the most reliable pile tests from a number of databases and were reviewed in depth to ensure that they had general consensus of the profession. The creation of the sand database has already led to the development of a new CPT-based method for driven piles in sand (Lehane et al. 2020) that has replaced the previously recommended earth pressure design

approach in the draft version of the next edition of ISO 19901-4, planned for publication in 2021.

This paper first presents an analysis of results from instrumented pile test data and numerical research that provide a rational basis for CPT-based formulations for axial pile capacity in clay and facilitate an understanding of the limitations of these formulations. The ability of a range of formulations to predict the capacities of piles in the "Unified" database is then examined to establish a final set of recommended equations for shaft friction and end bearing. The reliability of these equations is assessed by comparing their predictions for the capacities of piles in a separate "Test" database that was compiled for this study and with distributions of shaft frictions measured on well instrumented test piles.

Basis for formulation for shaft friction

General trends indicated by instrumented closed-ended piles

The stress changes that take place during the three stages in the life of a driven pile (i.e. installation, equalization and load testing) ultimately control the magnitude of the shaft friction that can be developed when a pile is in service. These changes are illustrated for the case of a lightly overconsolidated clay on Figure 1, which plots average data measured at the shaft of a jacked 6m long, 102mm diameter pile in Bothkennar clay (Lehane & Jardine 1994a). The trends shown in Figure 1 are typical of data measured in other instrumented pile tests reported by Azzouz & Morrison (1988), NGI (1988a,b) and Coop & Wroth (1989). The subscripts *i* and *c* used in the following refer to installation and following equalization (consolidation) respectively.

Figure 1a shows that radial stresses measured at any given depth during installation (σ_{ri}) are smaller than, but proportional to, the CPT q_t resistances. These σ_{ri} data also vary with the

distance of the radial stress sensor above the tip (*h*) and, in any given soil horizon, are about 40% of the q_t value at 4 pile diameters from the tip (h/D=4) and about 30% of q_t at h/D ≥14. Installation excess pore pressure ratios ($\Delta u_i/\sigma'_{v0}$) at this site varied from about 3 at h/D=1.5 to about 2.1 at h/D ≥ 16. After the pile reached the required embedment, as shown on Figure 1b, excess pore pressures dissipated, radial total stresses (σ_r) reduced and radial effective stresses increased (σ'_r) over several days to reach final fully equalized radial effective stress of σ'_{rc}. It is seen, for this example, that σ'_{rc} is about 3 times the radial effective stress acting on the shaft shortly after installation (σ'_{ri}). During load testing after full equalization, Figure 1c shows that radial effective stresses reduce to values at peak shear stresses (σ'_{rf}) that are about 20% less than σ'_{rc}. The maximum shaft friction (τ_f) is controlled, through Coulomb's friction law, by the radial effective stress at failure, σ'_{rf}, and the average clay-pile interface friction angle (δ) of 29°; this δ value is closely comparable to angles measured in ring interface shear tests on Bothkennar clay using a rough steel interface; see Lehane & Jardine (1992).

These stages in the life of a pile can be written in terms of radial total stresses (σ_r) normalized by the corrected cone resistance (q_t) using the following stress coefficients, where u_0 is the hydrostatic or ambient pore pressure:

$$S_i = (\sigma_{ri} - u_0)/q_t \quad (1)$$

$$S_c = (\sigma_{rc} - u_0)/q_t = \sigma'_{rc}/q_t \quad (2)$$

The loading coefficient is the ratio of the radial effective stress at peak shear stress (σ'_{rf}) to the equalized radial effective stress (σ'_{rc}):

$$f_L = \sigma'_{rf}/\sigma'_{rc} \quad (3)$$

Jardine et al. (2005), and many others, have confirmed the validity of Coulomb's friction law at the loading rates adopted in typical static load tests. Assuming Coulomb's friction law, Equations (1) to (3) then lead to the following expression for shaft friction (τ_f), which gives τ_f

as a direct function of the corrected cone resistance q_t, the three stress coefficients and the interface friction angle (δ):

$$\tau_f = \sigma'_{rf} \tan \delta = q_t \, S_i \, (S_c/S_i) \, f_L \tan \delta \quad (4)$$

The relationship between τ_f and q_t given in Equation (4) is examined first using data recorded for the Imperial College instrumented pile (ICP) in London clay, Cowden till, Bothkennar clay and Pentre clayey silt (Bond & Jardine 1991, Lehane & Jardine 1994a,b and Jardine et al. 2005). These experiments showed that the S_i measurements at each site could be represented as a unique function of the normalized distance above the pile tip (h/D) with the following format, where *A* and *c* are fitting parameters:

$$S_i = (\sigma_{ri} - u_0)/q_t = A \, (h/D)^{-c} \quad (5)$$

An illustration of the suitability of the format of Equation (5) is provided using data from Lehane & Jardine (1994b) in Figure 2 which reveals a clear similarity between the q_t profile measured in glacial till at Cowden, UK (Figure 2b) and corresponding ICP radial stress profiles recorded during installation by instruments located at h/D=4, 14 and 25 (Figure 2a). Radial stresses for the three piles installed from a 2.5m deep borehole vary by about 10% from mean values at any given instrument position. The range of all σ_{ri} data recorded by the four piles, presented as a variation of S_i with h/D, is shown on Figure 2c, which also plots the mean trend line (with correlation coefficient r^2=0.82) corresponding to the A and c coefficients provided in Table 1. Lehane (1992) shows that the equivalent variability about mean trend lines determined for σ_{ri} data for London clay and Bothkennar clay are 25% and 6% respectively.

Mean variations of S_i with h/D recorded by the ICP are plotted on Figure 3a, where considerable differences between the trends in each clay are apparent. The best-fit average values of *A* and *c* corresponding to these trend lines are provided in Table 1 and indicate a significant

dependence of '*c*' on clay type. The mean overconsolidation ratio (OCR) and plasticity index (I_p) at these sites are also provided in Table 1. A clear dependence of S_i on h/D was observed at a much reduced scale by Li & Lehane (2012) using a 9mm wide pile, confirming the suitability of pile diameter (or width) to normalize the distance from the pile tip (h).

The corresponding trends of normalized shaft friction, τ_f/q_t, are plotted on Figure 3b and were derived using Equation (4) and the mean A, c, S_c/S_i, f_L and δ values listed in Table 1, which were determined from the Imperial College experiments. These average coefficients did not indicate a systematic dependence on depth or pile length at the respective sites. It is evident that the spread of τ_f/q_t variations with h/D is lower than that of S_i in Figure 3a and τ_f/q_t ratios, at a fixed h/D, typically vary by less than 25% from the mean trend of the four clays.

Further instrumented pile test data are shown on Figure 4 to allow a comparison of results obtained in three lightly overconsolidated clays, namely Onsøy, Lierstranda and Bothkennar clays. The test results in both Onsøy and Lierstranda clays, which are reported in NGI (1988a), NGI (1988b) and Karlsrud et al. (1993), were obtained using eight 219mm diameter piles driven to final penetrations of between 15m and 35m. Each pile was equipped with a pair of radial stress sensors located at three levels, 5m apart. The CPT q_t profiles at Bothkennar and Onsøy varied approximately linearly with depth with a gradient of 40 kPa/m while q_t values at Lierstranda also varied linearly with depth but with a gradient of about 50 kPa/m.

Best-fit A and c coefficients derived from the measured S_i data are also listed in Table 1 and although these differ in magnitude, it is evident from the variations of S_i with h/D shown on Figure 4a that a broadly comparable S_i relationship with h/D exists for these three low OCR clays. However, as seen in Figures 4b and 4c, values of S_c/S_i and f_L are not similar with much lower values of these parameters being recorded in the Lierstranda clay.

Numerical analyses performed using the Strain Path Method (SPM) and the MIT-E3 constitutive model reported by Whittle & Baligh (1988), Azzouz et al. (1990), and others, have shown that clay sensitivity (S_t) and overconsolidation ratio (OCR) have a dominant effect on the relaxation of total stresses during pore pressure equalization and hence the S_c/S_i ratio. These analyses are supported by the measured ratios given in Table 1, which indicates S_c/S_i values between 0.8 and 1.0 in the high OCR Cowden till and London clay and between 0.15 and 0.43 in the three low OCR clays considered. Of particular note, is the much lower S_c/S_i value in Lierstranda clay. The CPT friction ratio data indicate that the Lierstranda clay has a sensitivity (S_t) of about 9 compared with S_t values of 3.5 and 6.0 for Bothkennar and Onsøy clays respectively. The CPT data for the Lierstranda clay plot close to or within Zone 1 of the soil behavior type (SBT) chart (Robertson 2009) denoting a sensitive clay while the Bothkennar and Onsøy clays classify as typical silty clays within Zone 3.

As seen in Table 1, the average f_L value for Lierstranda clay is also lower than for less sensitive clays, indicating that greater reductions in radial effective stress (σ'_r) occur during static load tests in this material. Greater reductions in σ'_r also occurred during undrained direct simple shear (DSS) tests on intact samples of Lierstranda clay compared with Onsøy and Bothkennar clays but these reductions were not as marked as those measured in the pile tests.

The compounding effect of low S_c/S_i and f_L ratios lead to very low τ_f/q_t ratios in Lierstranda clay, even though its S_i and δ values are comparable with the other low OCR clays. Such low ratios are apparent on Figure 5 which plots all variations of τ_f/q_t with h/D determined using equation (4) and the average coefficients in all clays (Table 1). The variations of τ_f/q_t with h/D are broadly similar, apart from in Lierstranda clay, and can be generally represented to within 20% by the following mean trend line, which is also shown on the figure :

$$\tau_f = 0.08\ q_t\ (h/D)^{-0.3} \qquad h/D > 0 \qquad (6)$$

The Lierstranda test data can be represented using the same format if a 'sensitivity factor', F_{st}, is applied to equation (6) i.e.

$$\tau_f = 0.08\, F_{st}\, q_t\, (h/D)^{-0.3} \qquad h/D > 0 \qquad (7)$$

where F_{st} =0.3 in Lierstranda clay (which is in Zone 1 of the SBT chart) and unity in 'typical' clays (i.e. in Zones 2, 3 and 4 of the SBT chart).

Equation (7), which was derived solely from instrumented pile tests, provides an indication of a potential formulation for a CPT-based method for closed-ended piles. However, when seeking a best-fit formulation to the Unified database of pile load tests, it is important to recognize that the similarity of the relationship for the soils with F_{st}=1.0 arises because of compensating effects in equation (4) of the parameters given in Table 1.

The dependence of τ_f on h/D in equation (7) is consistent with considerations of 'length effects' dating back to reduction of the adhesion factor (α) with L/D proposed by Semple et al. (1984) and Kolk & van der Velde (1996). Effects of progressive failure for long piles (e.g. Kraft 1981) come in addition to the h/D dependence in equation (7), which has been predicted numerically (but to a lesser extent) using the strain path method (SPM) with the MIT-E3 soil model (Whittle 1991). The effect of clay sensitivity, which emerges from the same SPM/MIT-E3 analyses, was employed explicitly in formulations for τ_f involving OCR proposed by Lehane et al. (1994) and Jardine et al. (2005).

Open-ended piles

The lower levels of soil displacement associated with the installation of open-ended piles compared to closed-ended piles might be expected to lead to lower shaft friction, as is the case for piles in sand (e.g. Gavin & Lehane 2003). However, empirical correlations such as proposed by Bustamante & Gianeselli (1982) and Karlsrud et al. (2005) suggest that there is no

dependence on the plugging condition in low OCR clays but that friction in stiff or high OCR clays can be lower for open-ended piles. Miller & Lutenegger (1997) also measured lower frictions for open-ended piles in high OCR clay and observed lower frictions at lower degrees of plugging during installation, where plugging was described by the plug length ratio (PLR).

Therefore, following a similar logic to that adopted for development of the CPT-based method for piles in sand using the Unified database (Lehane et al. 2020), effects of soil displacement can be examined in an extension of equation (5) by assuming that the normalized installation total stress (S_i) depends on h/D (as for a closed ended pile) and the effective area ratio (A_{re}):

$$S_i = A\ A_{re}^{b}\ (h/D)^{-c} \tag{8}$$

where *b* is a fitting parameter and A_{re} represents the relative degree of displacement compared to a closed-ended pile and is defined as a function of internal pile diameter (D_i) and PLR:

$$A_{re} = 1 - PLR\ (D_i/D)^2 = (D_{eq}/D)^2 \tag{9a}$$

$$PLR = \tanh\left[0.3\left(\frac{D_i}{d_{CPT}}\right)^{0.5}\right]; \quad d_{CPT} = 35.7mm \tag{9b}$$

PLR can be estimated from the equation (9b) which is based on available plugging data for piles in clay (Lehane et al. 2017) and is zero for closed-ended piles. The level of partial plugging of a pipe pile can also be described by the term D_{eq}, which is the diameter of an equivalent closed-ended pile leading to the same level of soil displacement.

Equation (8) is consistent with lateral stress data recorded in low OCR clay by Doherty & Gavin (2011) during installation of (one of the very few) instrumented pipe piles in clay. The same set of experiments showed that the values of S_c/S_i, f_L and δ were independent of the pile end condition. The potential effects on S_i of the clay OCR, referred to above, are not considered explicitly in the assessment of best-fit formulations due to the shortage of related information.

The pile design method proposed by Jardine & Chow (1996) employs the term D* to reflect the lower level of displacement induced during installation of a pipe pile, where :

$$D^* = (D^2 - D_i^2)^{0.5} \quad \text{for an open-ended pile}$$

$$D^* = D \quad \text{for a closed-ended pile} \tag{10}$$

The value of D* is equal to D_{eq} when PLR=1 and the corresponding expression to equation (8) is:

$$S_i = A\,(h/D^*)^{-c} \tag{11}$$

The format of equation (11) is consistent with numerical analyses performed by Chin (1986) who predicted similar strain fields around closed and (non-plugging) open-ended piles when distances from the pile are normalized by D^*. Xu et al. (2006) also show that the lateral stresses generated during installation of 1.02m diameter pipe piles and a 250mm square precast (closed-ended) pile have the same relationship with q_t and h/D^*. Equation (11) was therefore also examined in the calibration of the database as it represents a useful simplification of equation (8), noting that the approximate nature of the equation for PLR.

Loading direction coefficient, f_D

The loading direction coefficient, f_D, is defined as the ratio of the ultimate shaft friction developed in tension to that in compression. This coefficient is best assessed by comparing values of τ_f developed in first-time compression and tension load tests on identical piles. Such comparisons indicated f_D values of unity for piles in Kinnegar clay (McCabe and Lehane 2006), Bothkennar clay (Lehane & Jardine 1994a), London clay (Bond & Jardine 1991), Haga clay (Karlsrud and Haugen 1984) and Merville clay (Benzaria et al. 2012). However f_D values

measured in Cowden till (Lehane and Jardine 1994b) and Pentre clayey-silt (Chow 1997) were 0.8 and 1.1 respectively. On this basis, a best estimate f_D value of unity is adopted, although the optimization studies considered below also investigated other f_D values.

Basis for formulation for end bearing

The end bearing of compression piles in clay usually represents a small fraction of the total capacity. This low relative contribution is reflected by the scarcity of research into the end bearing of driven piles in clay, particularly pipe piles. API (2011) recommends taking the lesser of the internal friction (calculated using the same formulation for external friction) and the plugged end-bearing assumed to equal $9s_u$; this relationship equates to $0.75q_t$ for a typical CPT cone factor of 12, when relating cone resistance to undrained shear strength in triaxial compression. The plugged end bearing is almost always less than the calculated internal friction for typical piles with L/D > 5 and therefore the database analysis did not consider internal friction explicitly.

The few reliable cases that measured end bearing of closed-ended piles in clay indicate an end bearing at a pile movement of 10% of the pile diameter ($q_{b0.1}$) of about 80% of corrected cone resistance at the pile tip level (q_t). This proportion of q_t is similar to that proposed by Jardine & Chow (1996) and comparable to recommendations of API (2011) and Van Dijk & Kolk (2011).

Doherty and Gavin (2011) present a unique set of measurements involving a twin-walled instrumented pile that enabled separation of the average stress at the base of the plug and the stress on the annulus during pile installation. All installation data recorded can be represented by the following equation, where A_{re} is given by equation (9):

$$q_{b0.1} = [0.2 + 0.6\ A_{re}]\ q_t \qquad (12)$$

Equation (12) implies that the undrained end bearing capacity of a large offshore pile is approximately $0.2q_t$ (as A_{re} approaches zero) and is $0.8q_t$ for closed-ended piles. However, the capacities of piles in the unified database were measured in static load tests on relatively small diameter piles. Many of these pipe piles exhibited partial plugging during installation and also had a greater potential for drainage during the tests compared to closed-ended piles. Jardine et al. (2005) and Frank (2017) recommend $q_{b0.1}/q_t$ ratios for these smaller piles under load testing conditions of 0.4 and 0.35 respectively

On the basis of the foregoing, the following equations were considered to provide a reasonable estimate of the end bearing mobilized by the database piles in static load tests (noting that the mean contribution to compression capacity of end bearing of the database piles evaluated using these expressions was less than 15%):

$$q_{b0.1} = 0.8\ q_t \text{ (closed-ended pile)} \quad (13a)$$

$$q_{b0.1} = 0.4\ q_t \text{ (open-ended pile)} \quad (13b)$$

The Unified database

A full description of the "Unified" database in clay is provided in Lehane et al. (2017). A total of 300 pile load tests was examined but only 49 tests with CPT data were selected based on stringent selection criteria explained in Lehane et al. (2017). These criteria included: (i) piles had to be driven with a minimum diameter of 200mm and length of 5m, (ii) more than 75% of the shaft friction was provided by clay layers, (iii) good quality CPT data were available close to the pile test, (iv) the degree of consolidation prior to load testing was in excess of 80% and only first-time tests were considered, (v) load-displacement data were provided for each test pile up to a pile head displacement of D/10 and (vi) the loading rate was slow with ultimate capacity typically attained a number of hours after the test start. A "Test" database was

compiled for the present study and followed these key criteria apart from allowing jacked piles and piles with smaller diameters and shorter lengths.

Details of pile load tests in the Unified database are provided in Tables 2 and 4 while those for the test database are presented in Table 3. The tables give details on the pile configurations, end conditions, loading direction, equalization time (t_{eq}), maximum displacement rate during static load testing ($\dot{s}$), maximum measured axial capacity (Q_m) and measured capacity at a pile head displacement of 0.1D ($Q_{m,0.1D}$). The mean pile diameter of 450mm in the Unified database is significantly smaller than full scale offshore piles. However laboratory and centrifuge studies (e.g. Potts & Martins 1982, Li & Lehane 2012) have indicated that, unlike piles in sand, scale effects due to the diameter dependence of dilation at the shaft interface do not apply in clays. The database piles were load tested at periods after pile driving (t_{eq}) ranging from 21 to 130 days at stages when their degrees of excess pore pressure dissipation were assessed as being generally greater than 80% (see Lehane et al. 2017)

The measured pile capacity (Q_m) was taken as the load at a pile head displacement of 10% of the pile diameter ($Q_{m,0.1D}$) or the maximum measured load if this occurred at a lower displacement. The quoted values of Q_m are those arising from the resistance provided by the soil and exclude any contribution to resistance from the weight of piles or soil plugs. The unit shaft capacities assessed from the database test piles assumed that peak frictions (τ_f) operated over the entire pile shaft at the point of overall shaft failure and the formulations for τ_f calibrated from these test data are therefore conservative in the few cases where the long test piles experienced significant progressive softening at a displacement of 0.1D. Local shaft friction brittleness was generally small as indicated by the average database $Q_{m,0.1D}/Q_m$ ratio of 0.97 (see Table 4).

The base pressure mobilized is lower than the actual $q_{b0.1}$ value in cases when Q_m is greater than $Q_{0.1D}$. However this effect, as observed in the Unified database, is negligible as the base resistance typically represented only about 10% of a compression pile capacity and gains in base resistance between the displacement at maximum load (typically 5% of the diameter for the cases with $Q_m > Q_{0.1D}$) and 0.1D are low.

The creep rate ($\dot{s}$) recorded at maximum capacity for the piles in the Unified database varied in almost all cases between values of 0.2 and 1.0 mm/min. Creep rates are shown bracketed in Table 4 where they were not documented explicitly and needed to be estimated from the reported load test durations allowing for typical increases in creep rate as loading progresses. Load tests investigating the influence of displacement rate on capacity in high plasticity Bothkennar clay (Lehane & Jardine 1994a) showed that capacities differed by less than 5% when $\dot{s}$ varied between 0.05mm/min and 3mm/min but that viscous effects became more prominent at higher velocities (increasing shaft resistance by about 10% per log cycle increase in $\dot{s}$). The values of Q_m in the database may therefore be presumed to be insensitive to the range of creep rates that occurred in the load tests.

The soil properties in both the Unified and Test databases are summarized by presenting the median values in clay strata of the CPT consistency index (I_c), CPT friction ratio (F_r) and plasticity index (I_p) along the embedded lengths of the piles. Median values are employed as they provide more representative measures when there is significant layering at a given test site. These are plotted on the soil behavior type (SBT) chart on Figure 6 and on the plasticity chart on Figure 7. Figure 6 shows that the majority of the 31 clay sites fall within Zone 3 (silty clay to clay) and Zone 4 (clayey silt to silty clay) and are either lightly overconsolidated with normalized cone resistances (Q_{tn}) of 5 ± 3 or have high OCRs with Q_{tn} =35 ± 10. Two clays

(Pentre and West Delta) lie in Zone 2 (organic soils and clay) while three soils, namely Lierstranda, Sandpoint and Borsa clays lie close to or within Zone 1 (sensitive clays).

Figure 7 shows that the database comprises a large and uniform spread in I_p and liquid limit values, where all soils plot above (or just below) the A-line. It is interesting that, while the four clays classified in Zone 1 are of low plasticity (I_p <20%), the Pentre clay with a comparably low plasticity index (I_p=16%) plots in Zone 2 and has a measured sensitivity (S_t) of only of 1.5 (Chow 1997).

Optimization analyses

The instrumented pile test records showed that the dominant parameters controlling local shaft friction (τ_f) are the CPT resistance (q_t) and the length effect, as described by the h/D term. Initial calculations showed that use of the distance 'h' rather that the normalized value (h/D) provided less satisfactory fits to the data. Additional terms were also examined using the following two formats and assuming that the dependence of these terms could be represented as power functions (where C_1 and C_2 are constants):

$$\tau_f = C_1 \times q_t^a \times \sigma'^b_v \times (h/D)^{-c} \times A_{re}^d \times F_r^e \times I_c^f \times I_p^g \times f_D \times F_{st} \quad (14)$$

$$\tau_f = C_2 \times q_t^a \times \sigma'^b_v \times (h/D^*)^{-c} \times F_r^e \times I_c^f \times I_p^g \times f_D \times F_{st} \quad (15)$$

Parameters *a*, *b*, *c*, *d*, *e*, *f* and *g* are fitting parameters and a minimum h/D^* or h/D value was nominally taken equal to 1.0. Capacities were calculated for various combinations of these parameters using equation (13) to determine the base resistance of compression piles and assuming initially that τ_f could be represented as a product of the power functions. Equations (14) and (15) were used for calculation of τ_f in clay strata with I_c >2.5, while, in keeping with its recommendations, the new ISO 19901-4 CPT sand method (Lehane et al. 2020) was applied directly in sand and silty sand layers with I_c < 2.05. In (occasional) silt layers in the database

with I_c in the range between 2.05 and 2.5, the sand method was employed using the equivalent clean sand q_t value ($q_{t,sand}$), derived using the following relationship which is equivalent to the proposal of Robertson & Wride (1998) but adapted to a simplified format and modified to give a correction factor of unity at $I_c = 2.05$:

$$q_{t,sand} = [3.93\ I_c^2 - 14.78\ I_c + 14.78]\ q_t \quad \text{for } 2.05 < I_c < 2.5 \tag{16}$$

A spreadsheet-based optimization scheme was set up using the generalized reduced gradient approach (Baker 2011) to determine the combination of fitting parameters that minimized the coefficient of variation of the ratios of measured to calculated capacities (Q_m/Q_c) and gave an average Q_m/Q_c ratio of unity for all 49 piles in the Unified database. The spreadsheet results were verified independently using a Python code that used the Sequential Least Squares Programming (SLSQP) algorithm.

A variety of different constraints were applied to the variables to ensure that (i) the local minimum determined was a feasible solution, (ii) differences between calculated distributions of τ_f and those reported in available case histories were small (e.g. Figure 8) and (iii) the expression for τ_f was consistent with trends indicated in instrumented pile tests (Figure 5). Preliminary analyses examined trends of Q_m/Q_c values with respect to individual terms in equations (14) and (15) as well combinations of these terms (e.g. Figure 9). These analyses confirmed the general versatility of using power functions in assessing the relative impact of the terms and combinations of these terms.

Each Q_m/Q_c value was weighted following a procedure described in Lehane et al. (2017) to deduce a weighted coefficient of variation (CoV_w) for Q_m/Q_c ratios. Lower weightings were applied to multiple piles at the same site and the weightings also varied with the quality ratings assigned to each test pile by the team of experts responsible for compiling the database (Lehane

et al. 2017). Despite these procedures, the results of the analyses showed negligible differences between the statistics for weighted and unweighted coefficients of variation.

The analyses revealed the following key findings:

(i) The lowest CoV_w values were deduced when the exponent for q_t was unity and the exponent for σ'_v (see Equations 14 and 15) was close to zero. Consequently, unlike the α design method such as that recommended in API (2011), the analyses did not indicate a dependence of τ_f on q_t/σ'_v, which varies approximately with the undrained strength ratio and OCR. This characteristic is in keeping with the trends inferred from the instrumented pile tests on Figure 5.

(ii) For any combination of the fitting parameters, Q_m/Q_c ratios determined in three of the Zone 1 clays (and in particular the Lierstranda clay) were significantly over-predicted when F_{st} was assumed equal to unity. Consequently, optimization focused on pile tests in clays outside of Zone 1 and then re-visited the tests in Zone 1 to deduce recommendations for F_{st}.

(iii) Inclusion of the F_r and I_c terms in the formulation had no beneficial effect on the goodness-of-fit with the pile load tests in the Unified database i.e. optimized '*e*' and '*f*' parameters were effectively zero and the same best-estimate formulation was applicable to clays in Zones 2, 3 and 4 of the SBT chart.

(iv) The optimized exponent to I_p was close to zero indicating no effect of plasticity index on the best fit τ_f formulation. This finding contrasts with the strong dependence on I_p incorporated in the α method of Karlsrud et al. (2005).

(v) The minimum CoV_w values achieved using the function forms in equations (14) and (15) were identical and therefore equation (15), which uses the h/D* term, was adopted for simplicity. It is noted that equation (15) reduces to equation (14) if the exponent, *d*, of

the effective ratio (A_{re}) equals '-c/2'. The statistical analyses predicted *d* values that were close to -*c*/2 hence justifying use of equation (15).

(vi) Similar CoV_w values were obtained when f_D was varied between 0.85 and 1.15 indicating that f_D can be set equal to unity in line with the average parameter deduced from field tests discussed above.

(vii) CoV_w values showed marginal differences for 'c' varying between 0.15 and 0.3 (where c is the exponent for h/D^*). A '*c*' value of 0.25 was selected as it provided a slightly improved fit to the ultimate shear stress profiles recorded on test piles, especially large diameter pipe piles.

The initial, convenient assumption that the contribution of F_r, I_c and I_p to τ_f could be represented in the optimization analysis as the product of power functions of these terms was warranted because of the absence of any individual or combined contribution to the best-fit formulation. Consideration of the product of the q_t and σ'_v terms enabled an indirect check on the influence of undrained strength ratio while the inclusion in the formulation of the product of q_t with h/D or h/D* terms is consistent with the trend shown on Figure 5. Therefore, despite the wide-ranging investigation into potentially influential factors, the statistical analyses indicated that the following simple correlation for peak friction in tension and compression provided a best fit to the Unified database:

$$\tau_f = 0.07\, F_{st}\, q_t\ \ \mathrm{Max}[1, (h/D^*)]^{-0.25}$$

where $F_{st} = 1$ for clays in Zones 2, 3 and 4

$F_{st} = 0.5 \pm 0.2$ for Zone 1 clays (17)

It is encouraging that Equation (17) is almost identical to Equation (7) which was deduced independently from instrumented pile test data. The predictive performance of Equation (17)

for the Unified database is examined in terms of ratios of measured to calculated capacities (Q_m/Q_c) in Tables 4 and 5, where it is compared with predictions for the piles in the Unified database using six other published formulations for τ_f; further details are provided in Lehane et al. (2017). The statistics for Q_m/Q_c values provided in Table 4 are given in Table 5, which also lists the parameters employed in each of the τ_f formulations (noting contributions of base resistance to capacities were very small). It is evident that the mean Q_m/Q_c value for each formulation is close to unity but that the spread in predictions for Equation (17), as measured by the CoV for Q_m/Q_c (and hence its predictive reliability), is far less than the six other methods indicating a significantly higher level of reliability. The CoV values for Q_m/Q_c for the other methods are in the range of 0.3 to 0.6, which is consistent with the range quoted by Paikowsky et al. (2004) and Dithinde et al. (2011) for predictive methods in general.

The best-fit F_{st} values were 0.3 in Lierstranda clay and 0.7 in Borsa and Sandpoint clays. It is therefore evident that the analyses did not lead to a unique F_{st} value for Zone 1 clays and, as such, there is additional uncertainty related to use of the proposed F_{st} value of 0.5 for these clays. Consequently, pile capacities in Zone 1 soils need to be assessed with particular care and ideally rely on local experience and pile testing. In this regard, it is important to note that the measurement of CPT friction sleeve stress is prone to error and may lead to mis-classification of the soil type. Additional investigations to assist in a material's classification are recommended if the CPT data plot close to the Zone 1 boundary. It is also noteworthy that the CoV for Q_m/Q_c for Equation 17 excluding Zone 1 pile tests reduces to a value of 0.19 with a mean Q_m/Q_c of unity; CoV values show comparable reductions for the other methods included in Table 5 when Zone 1 pile tests are excluded.

The peak shear stress profiles calculated using equation (17) are compared on Figure 8 with profiles measured by three of the larger diameter pipe piles in the Unified database. It is seen that the profile for the very long pile in the soft clay at West Delta is well predicted while

predictions in the low OCR clay at Onsoy and high OCR clay at Tilbrook provide less precise matches to the measured distributions. While such differences may be partly attributed to errors in the friction inferred from measured axial load distributions and due to difficulties in separating end bearing and external friction for the compression pile at Tilbrook, the comparisons serve to highlight the approximate and empirical nature of equation (17).

The optimization analyses included a constraint to minimize the bias of Q_m/Q_c with respect to additional pile and soil parameters. To examine such bias, these ratios are plotted for the Unified database on Figure 9 against the pile diameter, pile slenderness ratio (L//D), the median friction ratio (F_r) and the median plasticity index (I_p). Best fit regression lines for each set of data indicate no clear dependence of Q_m/Q_c on L/D, F_r and I_p. The slight apparent trend seen on Figure 9a to overestimate pile capacity (i.e. Q_m/Q_c >1) as the diameter increases arises because of the two 1.5m diameter piles at Kansai (Matsumoto et al. 1992). These piles were driven into a clay deposit that included significant sand layers and, as such, their weighting to the overall statistics was relatively low in the analyses.

Equation (17) provides an expression for peak shaft friction that should be used in a load transfer analysis to determine the pile response under load. A load transfer analysis is also required to determine the capacity of long slender piles using t-z springs that include the post-peak softening 'branches' recommended by API (2011) or take account of other site-specific softening data. Such analyses were performed for the Unified database piles using the t-z curves documented in API (2011) and the average recommended softening coefficient of 0.8. The analyses had little effect on the evaluated Q_m/Q_c ratios for piles with L/D <50 but gave an increase in these ratios to values in excess of 0.75 for all piles with L/D>50 i.e. potential non-conservatism is reduced.

The shaft capacity of piles increases after consolidation is completed in a process referred to as ageing (e.g. Doherty & Gavin 2013). Equation (17) does not incorporate an ageing enhancement factor and provides a means of estimating shaft friction when the degree of excess pore pressure dissipation after driving is more than 80%. According to Teh & Houlsby (1991) and Randolph (2003), in a typical clay, achieving this level of dissipation at the shaft of a 2m diameter offshore pipe pile with a wall thickness of 40mm may take 6 months or longer while 80% dissipation for a 250mm square precast concrete pile would generally be complete in 3 to 4 weeks. It should also be noted that the development of dilative local shaft effective stress paths and other effects at low levels of equalization may compensate partially for low radial effective stresses with a consequence that partially equalized shaft frictions are often higher than anticipated from the degree of pore pressure dissipation e.g. Lehane & Jardine (1994a), Basu et al. (2013), Bittar et al. (2022).

The Test database, summarized in Table 3, was used to obtain an independent check of the best-fit formulation (equation 17) and involved an additional 8 clay types (all lying in Zones 3 and 4 on the SBT chart). Even though these piles were generally smaller in diameter and shorter than those in the Unified database, it was found that Equation (17) predicted the capacity relatively well with an average Q_m/Q_c value of 1.09 (i.e. slightly conservative in terms of predicted capacity) and a coefficient of variation for Q_m/Q_c of 0.22. Bias charts for the predictions of the Test database are provided on Figure 10 and demonstrate no obvious dependence of Q_m/Q_c on D, L/D or I_p but do display a tendency for Q_m/Q_c to reduce slightly with F_r. However, this trend was not evident from analysis of the Unified database, which comprises about 3 times more tests.

The statistics for the Test database are consistent with those of the Unified database and provide additional evidence in support of the general applicability of Equation (17). It is of note that the outlier Q_m/Q_c values in the Test database occurred for the piles in Bothkennar and London

clay and averaged 1.5 and 0.67 respectively. These relatively large deviations from the average, which are also evident on Figure 5, partially reflect the relatively high δ value of 29° in Bothkennar clay and relatively low δ value of 13° in London clay and suggest that improvements of predictive performance in future correlations may be achieved if δ values are measured and documented reliably for new test piles. The variability of Q_m/Q_c on Figures 9 and 10 is a simple consequence of the limitations of the CPT-based formulation and the variability in the pile load test results.

Conclusions

This paper presents the development of a new CPT based method for assessment of the axial capacity of driven piles in clay. Equation (12) provides the expression deduced for the ultimate end bearing capacity (defined at a displacement of 10% of the pile diameter) while the expression for the peak local shaft friction is given in Equation (17); these equations are valid for soil falling within zones 2, 3 and 4 of soil behavior chart and are applicable at slow rates of loading (typical of static load tests) after equalization of excess pore pressures. The equations are consistent with findings from field research and numerical analyses and were calibrated using the Unified database of pile load tests published in Lehane et al. (2017). The method is a significant improvement on popular existing methods and shown to provide good predictions for both the Unified database and an additional Test database that was compiled to enable an independent check of the method. Measured ultimate shaft friction distributions are also seen to be reasonably well estimated. While providing generally good predictions for the particular database used for its calibration, its empirical formulation is recognized and designers should exercise due caution with the approach, especially when considering sensitive clays.

Data availability statement

All data and models used during the study appear in the submitted article.

Acknowledgements

The authors gratefully acknowledge the funding and support provided under a Joint Industry Project (JIP) funded by Aramco, Equinor, Lundin, Ørsted, ONGC, BP, Total, ExxonMobil, EnBW, EDF and SSER. The significant contribution of Dr. Jit Kheng Lim to the database compilation is also highly appreciated as are the technical contributions of the JIP steering committee members to the development of the method.

Notation

The following symbols and abbreviations are used in this paper:

A_{re} effective area ratio (Ratio of soil displaced by pipe pile to displacement by closed-ended pile)

c exponent to h/D and h/D*

CoV coefficient of variation

CoV_w weighted coefficient of variation

CPT Cone Penetration Test

d_{CPT} diameter of a standard cone penetrometer

D pile diameter

D_{eq} diameter of an equivalent closed-ended pile that induces the sane soil displacement during installation as a pipe pile

D_i inner pile diameter (of pipe pile)

D* D_{eq} value for full coring pipe pile or D for closed-ended pile

f_D load direction coefficient for shaft friction

f_L loading coefficient ($\sigma'_{rf}/ \sigma'_{rc}$)

F_{st} sensitivity coefficient

F_r CPT friction ratio

h height of given point on shaft above the pile base

ICP Imperial College instrumented pile

I_c CPT soil consistency index

I_p plasticity index

JIP joint industry project

L pile length

OCR overconsolidation ratio

PLR plug length ratio (=plug length divided by embedded pile length)

$q_{b0.1}$ end bearing stress at a pile base displacement of D/10

q_c cone resistance

q_t cone resistance corrected for pore pressure at filter

q_{net} net cone resistance= $q_t-\sigma_{v0}$

$q_{t,sand}$ q_t measured at drained rate of penetration in silt

Q_{tn} normalized cone resistance (see Robertson 2009)

Q_c Calculated pile capacity

Q_m measured pile capacity (defined at s=0.1D if not attained at lower s)

$Q_{m,0.1D}$ measured pile head load at s=0.1D

s_u^{UU} triaxial compression unconsolidated undrained (UU) shear strength

s Pile head displacement in load test

$\dot{s}$ maximum pile displacement rate in static load test

s_{max} Pile head displacement at Q_m

SBT soil behavior type

SPM strain path method

t_{eq} time between installation and load testing

u_0 ambient (hydrostatic) pore pressure

α adhesion factor (τ_f / s_u^{UU})

δ clay-pile interface friction angle

μ Mean value of Q_m/Q_c

Δu_i excess pore pressure at pile shaft during installation

σ_{rc},σ'_{rc} radial total and effective stress after equalisation of pore pressure

σ_{ri}, $\sigma'_{ri,}$ radial total and effective stress operating during installation

σ'_{rf} radial effective stress at peak shear stress in load test

σ'_{v0} in-situ vertical effective stress

τ_f peak shear stress

References

Almeida, M.S., Danziger, F.A., and Lunne, T. (1996). Use of the piezocone test to predict the axial capacity of driven and jacked piles in clay. Canadian Geotechnical J., 33(1): 23-41.

API. (2011). ANSI/API RP 2GEO: Geotechnical and Foundation Design Considerations. ISO 19901-4:2003 (Modified), Petroleum and natural gas industries-Specific requirements for offshore structures, Part 4-Geotechnical and foundation design considerations. 1st edition. Washington, DC: API Publishing Services.

Azzouz, A.S., Baligh, M.M. and Whittle, A.J. (1990). Shaft Resistance of Piles in Clay. Journal of Geotechnical Engineering, 116(2): 205–221.

Azzouz, A.S., and Morrison, M.J. (1988). Field Measurements on Model Pile in Two Clay Deposits. J. Geotechnical Engineering, ASCE, 114(1): 104–121.

Baker K.R. (2011). Optimization modelling with spreadsheets. Wiley Online library.

Basu, P., Prezzi, M., Salgado, R. and Chakraborty T. (2014). Shaft resistance and setup factors for piles jacked in clay. J. Geotech. & Geoenv. Engrg, ASCE, 140 (3), 57-73.

Benzaria, O., Puech, A. and Kouby, A. Le. (2012). Cyclic axial load tests on driven piles in overconsolidated clay. Offshore Site Investigation and Geotechnics 2012: Integrated Technologies - Present and Future, OSIG 2012: 307–314.

Bittar, E., Huang, B., Lehane, B.M. and Watson, P (2022). Pile ageing to support life extension of offshore platforms. Proc 20th Int. Conf. Soil Mech. Geotech. Engrg, Sydney (in press)

Bond, A.J. (1989). Behaviour of displacement piles in overconsolidated clays. PhD thesis, Imperial College London (University of London).

Bond, A.J. and Jardine R.J. (1991). Effects of installing displacement piles in high OCR clay. Geotechnique, 41(3), 341-363.

Bustamante, M. and Gianeselli, L. (1982). Pile Bearing Capacity Prediction by Means of Static Penetrometer CPT. Proceedings of the Second European Symposium on Penetration Testing:

493–500.

Chin, C.T. (1986). Open-ended pile penetration in saturated clays. PhD thesis, Massachusetts Institute of Technology, Boston, MA.

Chow, F. (1997). Investigations into the behaviour of displacement piles for offshore foundations. PhD thesis, Imperial College London (University of London).

Coop, M.R. and Wroth, C.P. (1989). Field studies of an instrumented model pile in clay. Geotechnique, 39(4): 679–696.

Van Dijk, B.F.J. and Kolk, H.J. (2011). CPT-based design method for axial capacity of offshore piles in clays. *In* Proc. of the Int. Symposium on Frontiers in Offshore Geotechnics II. Edited by S. Gourvenec and D. White. Taylor & Francis Group, London. pp. 555–560.

Doherty, P. and Gavin, K. (2011). Shaft Capacity of Open-Ended Piles in Clay. J. Geotech. & Geoenv. Engrg, 137(11): 1090–1102.

Doherty, P. and Gavin, K. (2013). Pile Aging in cohesive soils. J. Geotech. & Geoenv. Engrg., ASCE, 139(9):1620-1624.

Dithinde, M., Phoon K.K., De Wet M. and Retief J.V. (2011). Characterization of Model Uncertainty in the Static Pile Design Formula. J. Geotech. & Geoenv. Engrg, ASCE, 137 (1), 70-85.

Eslami, A. and Fellenius, B.H. 1997. Pile capacity by direct CPT and CPTu methods applied to 102 case histories. Canadian Geotechnical J., 34(6): 886–904.

Frank, R. 2017. Some aspects of research and practice for pile design in France. Innovative Infrastructure Solutions, 2(1): 1–15. Springer International Publishing.

Gavin, K.G. and Lehane, B.M. (2003). Shaft friction for open-ended piles in sand. Canadian Geotechnical J., 40(1), 36-45.

ISO 19901-4. Petroleum and natural gas industries- Specific requirements for offshore structures, Part 4: Geotechnical and foundation design considerations. International

Standards Organisation; 1996 edition to be updated to 2021 edition.

Jardine, R., and Chow, F. 1996. New design methods for offshore piles. Marine Technology Directorate, London, UK.

Jardine, R., Chow, F., Overy, R. and Standing, J. (2005). ICP Design Methods for Driven Piles in Sands and Clays. Thomas Telford London.

Karlsrud, K., Clausen, C.J.F. and Aas, P.M. (2005). Bearing capacity of driven piles in clay, the NGI approach. Proc. Int. Symp. on Frontiers Offshore Geotechnics, Perth. pp. 775–782.

Karlsrud, K. and Haugen, T. (1985). Axial static capacity of steel model piles in over-consolidated clay. Proc., 11th Int. Conf. on Soil Mechanics and Foundation Engineering, Vol. 3, Balkema, Rotterdam, Netherlands, 1401–1406.

Karlsrud, K., Kalsnes, B. and Nowacki, F. (1993). Response of piles in soft clay and silt deposits to static and cyclic axial loading based on recent instrumented pile load tests. *In* Offshore Site Investigation and Foundation Behaviour. Springer. pp. 549–583.

Kolk, H. and van der Velde, E. (1996). A Reliable Method to Determine Friction Capacity of Piles Driven into Clays. *In* Proc. Offshore Technology Conference (OTC), Houston, Texas, Pub No. 413532.

Lehane, B.M. (1992). Experimental investigations of pile behaviour using instrumented field piles. PhD thesis, Imperial College London (University of London).

Lehane B.M. and Jardine R.J. (1992). On the residual strength of Bothkennar clay. *Geotechnique*, 42(2), 363-368.

Lehane, B.M., Liu, Z., Bittar, E., Nadim, F., Lacasse, S., Jardine, R., Carotenuto, P., Rattley, M., Jeanjean, P., Gavin, K., Gilbert, R., Bergan-haavik, J. and Morgan, N. (2020). A new CPT-based axial pile capacity design method for driven piles in sand. Proc. 5th Int. Symp. Frontiers Offshore Geotechnics, ISFOG-21, Paper No. 3457. DFI publications, New Jersey.

Lehane B.M., Chow F.C., McCabe B.M. and Jardine R.J. (2000). Relationships between shaft

capacity of driven piles and CPT end resistance. *Geotech. Engrg.*, ICE, 143, 93-101.

Lehane, B.M. and Jardine, R.J. (1994a). Displacement-pile behaviour in a soft marine clay. Canadian Geotechnical J., 31(2):181-191.

Lehane, B.M. and Jardine, R.J. (1994b). Displacement pile behaviour in glacial clay. Canadian Geotechnical J., 31(1): 79-90.

Lehane, B.M., Jardine, R.J., Bond, A.J. and Chow, F.C. (1994). The development of shaft resistance on displacement piles in clay. *In* International conference on soil mechanics and foundation engineering. pp. 473–476.

Lehane, B.M., Li, Y. and Williams, R. (2013). Shaft Capacity of Displacement Piles in Clay Using the Cone Penetration Test. J. Geotech. & Geoenv. Engrg., ASCE, 139(2):253-266.

Lehane, B.M., Lim, J.K., Carotenuto, P., Nadim, F., Lacasse, S., Jardine, R.J. and van Dijk, B.F.J. (2017). Characteristics of Unified Databases for Driven piles. Proc. 8th International Conf. Offshore investigation and Geotechnics: Smarter solutions for offshore developments, Society for Underwater Technology, 1, 162-194.

Li Y. and Lehane B.M. (2012). Insights gained from instrumented centrifuge displacement piles in Kaolin. Int. Journal of Geotechnical Engineering, 6, 157-161.

Matsumoto, T., Sekiguchi, H., Shibata, T. and Fuse, Y. (1992). Performance of steel pipe piles driven in Pleistocene clays. *In* International conference on the application of stress-wave theory to piles. pp. 293–298.

McCabe, B.A. and Lehane, B.M. (2006). Behavior of axially loaded pile groups driven in clayey silt. J. Geotech. and Geoenv. Engrg, ASCE, 132(3): 401–410.

Miller, G.A. and Lutenegger, A.J. (1997). Influence of pile plugging on skin friction in overconsolidated clay. J. Geotechnical Engineering, ASCE, 123(6): 525–533.

Niazi, F.S. and Mayne, P.W. (2016). CPTu-based enhanced UniCone method for pile capacity. Engineering Geology, 212: 21–34. Elsevier B.V.

Norwegian Geotechnical Institute (NGI). (1988a). Summary, interpretation and analysis of the pile load tests at the Lierstranda test site. NGI Rep. 52523-26, Oslo, Norway.

Norwegian Geotechnical Institute (NGI). (1988b). Summary, interpretation and analysis of the pile load tests at the Onsoy test site. NGI Rep.52523-23, Oslo, Norway.

Potts, D.M. and Martins J.P. (1982). The shaft resistance of axially loaded piles in clay. Géotechnique 32(4): 269-386.

Paikowsky S.G., Birgisson B., McVay M., Nguyen T., Kuo C., Baecher G., Ayyub B., Stenerssen K., O'Malley K, Chernauskas L., O'Neill M. (2004). Load and resistance factor, Design (LFRD) for deep foundations. NCHRP Report 507, Transport Research Board, Washington D.C.

Randolph, MF. (2003). Science and empiricism in pile foundation design. Géotechnique 53(10): 847-876.

Randolph, M. F., and Murphy, B. S. (1985). Shaft capacity of driven piles in clay. Proc., Offshore Technology Conf., Offshore Technology Conference, Houston.

Robertson, P.K. 2009. Interpretation of cone penetration tests - A unified approach. Canadian Geotechnical J., 46(11):1337-1355.

Robertson, P.K., and Wride, C.E. (1998). Evaluating cyclic liquefaction potential using the cone penetration test. Canadian Geotechnical Journal, 35(3):442-459.

Semple, R.M., Rigden, W.J., Randolph, M.F. and Murphy, B.S. (1984). Shaft capacity of driven pipe piles in clay. Proc. Symp. On Codes and Standards, ASCE National Conv., San Francisco. pp. 59–79.

Shanghai Xian Dai Architectural Design Co Ltd. (2008). The research on single piles bearing capacity methods in Shanghai. Shanghai Construction and Transportation Commission Marketing Dept Report 2007-02, Dec 2008.

Teh, CI and Houlsby, GT. (1991). An analytical study of the cone penetration test in clay.

Géotechnique 41(1): 17-34.Whittle, A.J. and Baligh, M.M. (1988). A Model for Predicting the Performance of TLP Piles in Clays. Final Report Phase III to sponsors, Dept. of Civil Engineering, Massachusetts Institute of Technology.

Whittle, A.J. (1991). Predictions of instrumented pile behaviour at the Bothkennar site. Report for Dept. of Civil Engineering, Imperial College London (summarised in Lehane 1992).

Xu, X., Liu, H. and Lehane, B.M. (2006). Pipe pile installation effects in soft clay. Proceedings of the Institution of Civil Engineers: Geotechnical Engineering, ICE, 159(4):285-296.

Table 1 Coefficients measured in instrumented pile tests

Clay	OCR	I_p (%)	A	c	S_c/S_i	f_L	δ (degs)
Cowden till	10	21	0.40	0.36	0.80	0.80	22
London Clay	30	50	0.65	0.59	1.00	1.00	13
Bothkennar clay	1.7	47	0.50	0.24	0.43	0.80	29
Pentre silt	1.8	16	0.62	0.45	0.65	0.92	20
Onsoy Clay	1.3	43	0.40	0.15	0.32	0.81	24
Lierstranda clay	1.2	16	0.48	0.28	0.15	0.60	26.5

Definitions of coefficients are provided in Equations (1), (2), (3) and (5)

Table 2**.** Details of pile tests in Unified database

N	Site	Test	Type	Borehole depth (m)	Tip depth (m)	t_{eq} (days)	D (m)	D_i (m)	L/D	Reference
1	Onsoy	A1-02	CET	5.0	15	26	0.22		45.7	Karlsrud et al. (1993b); NGI (1988b)
2	Onsoy	A3-02	CET	20.0	30	54	0.22		45.7	Karlsrud et al. (1993b); NGI (1988b)
3	Onsoy	B1-02	OET	5.0	15	81	0.81	0.79	12.3	Karlsrud et al. (1993b); NGI (1988b)
4	Onsoy	C1-02	CET	5.0	35	50	0.22		137.0	Karlsrud et al. (1993b); NGI (1988b)
5	Onsoy	C2-02	CET	5.0	35	51	0.22		137.0	Karlsrud et al. (1993b); NGI (1988b)
6	Lierstranda	A7-02	CET	5.0	15	29	0.22		45.7	Karlsrud et al. (1993b); NGI (1988a)
7	Lierstranda	A8-02	CET	12.5	22.5	32	0.22		45.7	Karlsrud et al. (1993b); NGI (1988a)
8	Lierstranda	A9-02	CET	20.0	30	31	0.22		45.7	Karlsrud et al. (1993b); NGI (1988a)
9	Lierstranda	A10-02	CET	27.5	37.5	30	0.22		45.7	Karlsrud et al. (1993b); NGI (1988a)
10	Lierstranda	B2-02	OET	5.0	15	52	0.81	0.79	12.3	Karlsrud et al. (1993b); NGI (1988a)
11	Pentre	A6-02a	CET	25.0	32.5	32	0.22		34.2	Karlsrud et al. (1993a, b); NGI (1988c); Lambson et al. (1993)
12	Pentre	LDP	OEC	15.0	55	44	0.76	0.73	52.5	Gibbs et al. (1993); Cox et al. (1993a, b); Lambson et al. (1993)
13	Tilbrook	A1	CET	3.0	12.9	61	0.22		45.2	Karlsrud et al. (1993a); NGI (1989c); Lambson et al. (1993)
14	Tilbrook	B1	CET	17.5	25.6	59	0.22		37.0	Karlsrud et al. (1993a); NGI (1989c); Lambson et al. (1993)
15	Tilbrook	C1	CET	3.0	17.5	59	0.22		66.2	Karlsrud et al. (1993a); NGI (1989c); Lambson et al. (1993)
16	Tilbrook	D1	OET	3.0	17.5	73	0.27	0.24	53.1	Karlsrud et al. (1993a); NGI (1989c); Lambson et al. (1993)

Table 2 (continued). Details of pile tests in Unified database

N	Site	Test	Type	Borehole depth (m)	Toe depth (m)	t_{eq} (days)	D (m)	D_i (m)	L/D	Reference
17	Tilbrook	LDP-C	OEC	0.0	30	130	0.76	0.70	39.4	Gibbs et al. (1993); Cox et al. (1993a, b); Lambson et al. (1993)
18	Cowden	A	OEC	0.0	9.2	30	0.46	0.42	20.1	Ridgen et al. (1979); Gallagher & St. John (1980)
19	Cowden	B	CEC	0.0	9.2	30	0.46		20.1	Ridgen et al. (1979); Gallagher & St. John (1980)
20	AquaticPark	S2-1	OET	57.9	80.5	60	0.76	0.69	29.7	Pelletier & Doyle (1982); Doyle & Pelletier (1985)
21	Kinnegar	S1	CEC	0.0	6	82	0.25		24.0	McCabe & Lehane (2006); HSE (2003)
22	Kinnegar	S2	CET	0.0	6	99	0.25		24.0	McCabe & Lehane (2006); HSE (2003)
23	Kontich	B	OEC	1.5	23.5	21	0.61	0.56	36.1	Heerema (1979); De Beer et al. (1974, 1977)
24	Kansai	T1a	OEC	0.0	32.8	35	1.50	1.46	21.9	Matsumoto et al. (1992); Shibata et al. (1989); Akai et al. (1991)
25	Kansai	T2	OEC	0.0	48.3	42	1.50	1.46	32.2	Matsumoto et al. (1992); Shibata et al. (1989); Akai et al. (1991)
26	SintKatelijne	A1	CEC	1.0	7.4	92	0.35		18.3	Charue et al. (2001); Huybrechts (2001); Menge (2001)
27	SintKatelijne	A4	CEC	1.0	11.6	89	0.35		30.3	Charue et al. (2001); Huybrechts (2001); Menge (2001)
28	Sandpoint	p	CEC	0.0	45.9	48	0.41	0.38	113.1	Fellenius et al. (2004)
29	WestDelta	LS1	OET	0.0	71.3	116	0.76	0.72	93.6	Bogard & Matlock (1998); Audibert & Hamilton (1998); Ertec (1982); NGI (1989b)
30	Onsoy2	O1-1	OET	1.4	19.1	78	0.51	0.50	34.8	Karlsrud et al. (2014); NGI (2013)
31	Cowden2	C2-1	OET	1.0	10	119	0.46	0.43	19.7	Karlsrud et al. (2014); NGI (2013); Powell & Butcher (2003)

Table 2 (continued). Details of pile tests in Unified database

N	Site	Test	Type	Borehole depth (m)	Toe depth (m)	t_{eq} (days)	D (m)	D_i (m)	L/D	Reference
32	Femern	F2-1	OET	0.0	25	34	0.51	0.47	49.2	Karlsrud (2012); Femern A/S (2014)
33	Stjordal	S2-1	OET	1.0	23.6	50	0.51	0.50	44.5	Karlsrud et al. (2014); NGI (2013)
34	Merville	D1	OEC	0.0	9.4	44	0.51	0.48	18.5	Rocher-Lacoste et al. (2003); Ma & Holeyman (2003)
35	Merville2	B1S1	CEC	4.0	13	57	0.41		22.2	Benzaria et al. (2012); Puech & Benzaria (2013)
36	Merville2	B3S1	CET	4.0	13	62	0.41		22.2	Benzaria et al. (2012); Puech & Benzaria (2013)
37	Klang	TP1A	OEC	0.0	35.5	26	0.25	0.14	142.0	Liew & Kwong (2015)
38	Riau	G1-T1	OEC	0.0	24	73	0.35	0.20	68.6	Liew et al. (2002)
39	Riau	G10-T1	OEC	0.0	30	71	0.35	0.20	85.7	Liew et al. (2002)
40	Riau	G6-T1	OEC	0.0	36	68	0.35	0.20	102.9	Liew et al. (2002)
41	GoldenEars	SC	CEC	0.0	36	120	0.36		100.8	Amini et al. (2008)
42	LuluIsland	UBC1	CEC	2.0	14.3	82	0.32		38.0	Robertson et al. (1988); Robertson et al. (1985); Davies (1987)
43	Borsa	P1&2	OET	0.0	50	63	0.41	0.38	123.2	Aas-Jakobsen (2003a); Karlsrud (2012)
45	Quebec	9	CET	2.3	18.1	66	0.32		49.5	Fellenius & Samson (1976)
46	Maskinonge	p3	CEC	0.0	23.8	58	0.23		103.5	Blanchet et al. (1980)
47	Maskinonge	p4	CEC	0.0	23.8	58	0.22	0.21	108.7	Blanchet et al. (1980)
48	Maskinonge	p5	CEC	0.0	37.5	58	0.23		163.0	Blanchet et al. (1980)
49	Goteborg	a	CEC	2.0	18	34	0.24		68.1	Bengtsson & Sallfors (1983)

Table 3 Details of pile tests in Test database

N	Site	Test	Type	Borehole depth (m)	Toe depth (m)	t_{eq} (days)	D (m)	D_i (m)	L/D	Q_m (MN)	Q_c (MN)	Q_m/Q_c	Reference
50	Bayswater	4	OET	1.1	6.2	3	0.17	0.16	30.9	0.038	0.026	1.45	Bittar et al. (2022)
51	CanonsPark	CP5f_L1T	CET	2.1	6	2	0.10		38.2	0.101	0.094	1.07	Bond (1989); Bond & Jardine (1995)
52	Gloucester	A1	CET	1.0	3	30	0.10		20.0	0.006	0.006	1.05	McQueen et al. (2015); Hosseini & Rayhani (2017)
53	Gloucester	B1	CET	1.0	3	30	0.10		20.0	0.006	0.006	0.96	McQueen et al. (2015); Hosseini & Rayhani (2017)
54	Gloucester	C1	OET	1.0	3	30	0.10	0.09	20.0	0.005	0.005	1.08	McQueen et al. (2015); Hosseini & Rayhani (2017)
55	Haga	2	CET	0.2	5.15	20	0.15		32.4	0.055	0.067	0.82	Karlsrud & Haugen (1985)
56	StAlban	A_3	CET	1.5	7.6	20	0.22		53.9	0.085	0.066	1.29	Roy et al. (1981); Konrad & Roy (1987)
57	Bothkennar	BK2_L1C	CEC	1.2	6	4	0.10		103.9	0.025	0.017	1.50	Lehane (1992)
58	CanonsPark	AL1C	CEC	3.0	6.5	31	0.17		27.6	0.159	0.255	0.62	Wardle et al. (1992)
59	CanonsPark	BL1C	CEC	2.0	6.5	74	0.17		47.1	0.194	0.272	0.71	Wardle et al. (1992)
60	Cowden	193o	OEC	0.8	9.5	1	0.19	0.18	20.6	0.584	0.368	1.59	Ponniah (1989)
61	Cowden	CW2_L1C	CEC	2.7	6.35	4	0.10		26.5	0.124	0.102	1.22	Lehane (1992)
62	Hangzhou	T2	OEC	0.0	13	17	0.40	0.25	45.1	1.200	0.860	1.40	Kou et al. (2018)
63	Kinnegar	OE1	OEC	2.0	4.04	5	0.17	0.15	36.3	0.012	0.009	1.30	Doherty & Gavin (2011)
64	Pentre	PT3L1T	CET	12.0	17.47	0.7	0.10		32.5	0.075	0.055	1.36	Chow (1996)
65	Pentre	PT5L1T	CET	8.1	18.73	3	0.10		12.0	0.126	0.093	1.35	Chow (1996)
66	Pentre	PT1L1C	CEC	10.5	14.8	0.6	0.10		42.2	0.035	0.045	0.78	Chow (1996)
67	Pentre	PT2L1C	CEC	10.5	19	3	0.10		83.3	0.082	0.092	0.89	Chow (1996)
68	Pentre	PT4L1C	CEC	8.1	14.02	1	0.10		57.6	0.064	0.061	1.06	Chow (1996)
69	Pentre	PT6L1C	CEC	10.2	14	3	0.10		37.3	0.043	0.042	1.03	Chow (1996)
70	Shanghai	159	CEC	0.0	23	3	0.25		92.0	0.620	0.587	1.06	Shanghai Xian Dai (2008)
71	Shanghai	f5	CEC	0.0	22	3	0.25		88.0	0.570	0.709	0.80	Shanghai Xian Dai (2008)
72	Shanghai	p5	CEC	0.0	24	3	0.25		96.0	0.720	0.625	1.15	Shanghai Xian Dai (2008)
73	Shanghai	s73	CEC	0.0	24	3	0.25		96.0	0.915	0.845	1.08	Shanghai Xian Dai (2008)

Table 4. Measured and calculated capacities in Unified database

								Q_m/Q_c						
N	**Site**	**Test**	**Type**	**Q_m (MN)**	**$Q_{m,0.1D}$ (MN)**	**s_{max} (mm)**	**$\dot{s}$ (mm/min)**	**API-11**	**Fugro-96**	**ICP-05**	**NGI-05**	**UWA-13**	**Fugro-10**	**Eqn. 17**
1	Onsoy	A1-02	CET	0.091	0.091	5	0.7	0.85	1.00	0.51	0.90	0.97	0.72	0.74
2	Onsoy	A3-02	CET	0.224	0.224	11	0.6	0.98	1.16	0.63	1.02	1.13	0.89	0.89
3	Onsoy	B1-02	OET	0.427	0.427	8	0.4	1.01	1.06	0.67	1.20	1.29	0.92	0.99
4	Onsoy	C1-02	CET	0.407	0.407	16	1	0.81	1.01	0.54	0.76	0.99	0.81	0.81
5	Onsoy	C2-02	CET	0.487	0.487	13	0.4	0.97	1.21	0.65	0.91	1.18	0.97	0.97
6	Lierstranda	A7-02	CET	0.069	0.069	2	0.5	0.47	0.54	0.23	0.63	0.51	0.36	0.70
7	Lierstranda	A8-02	CET	0.077	0.077	6	0.3	0.35	0.42	0.21	0.59	0.43	0.32	0.64
8	Lierstranda	A9-02	CET	0.1	0.1	15	0.9	0.34	0.41	0.20	0.71	0.43	0.33	0.68
9	Lierstranda	A10-02	CET	0.074	0.074	6	0.5	0.20	0.24	0.12	0.47	0.26	0.20	0.49
10	Lierstranda	B2-02	OET	0.26	0.26	8	0.2	0.45	0.46	0.24	0.64	0.54	0.37	0.75
11	Pentre	A6-02a	CET	0.351	0.351	20	0.4	0.96	1.12	0.60	1.74	1.21	0.81	0.94
12	Pentre	LDP	OEC	6.32	5.8	35	1	0.72	0.81	0.63	1.03	1.35	0.95	1.14
13	Tilbrook	A1	CET	1.246	1.246	15	1	1.29	1.21	1.35	1.10	1.00	1.22	0.98
14	Tilbrook	B1	CET	1.741	1.741	7	1	1.33	1.22	2.00	1.23	1.18	1.18	0.93
15	Tilbrook	C1	CET	2.045	2.045	16	1	1.41	1.34	1.50	1.16	1.05	1.27	0.82
16	Tilbrook	D1	OET	2.039	2.039	9	1	1.10	1.03	1.32	1.07	0.93	1.02	0.74

Table 4**.** Measured and calculated capacities in Unified database (continued)

								Q_m/Q_c						
N	**Site**	**Test**	**Type**	Q_m **(MN)**	$Q_{m,0.1D}$ **(MN)**	s_{max} **(mm)**	$\dot{s}$ **(mm/min)**	**API-11**	**Fugro-96**	**ICP-05**	**NGI-05**	**UWA-13**	**Fugro-10**	**Eqn. 17**
17	Tilbrook	LDP-C	OEC	16.5	15.2	28	1	1.09	0.99	1.75	1.09	1.10	1.22	1.05
18	Cowden	A	OEC	1.18	1.18	24	1.5	1.46	1.29	1.11	1.53	1.21	1.13	1.09
19	Cowden	B	CEC	1.42	1.39	20	1.5	1.76	1.55	1.06	1.71	1.12	1.36	1.01
20	AquaticPark	S2-1	OET	10.5	10.5	6	-	0.85	0.88	0.84	1.28	1.28	1.02	1.01
21	Kinnegar	S1	CEC	0.073	0.073	15	0.8	0.75	0.71	0.93	0.76	1.12	0.90	1.04
22	Kinnegar	S2	CET	0.065	0.065	20	0.8	0.85	0.80	1.07	0.81	1.37	0.99	1.17
23	Kontich	B	OEC	5.07	4.5	16	1.3	1.43	1.26	2.34	1.42	1.29	1.16	1.06
24	Kansai	T1a	OEC	9.47	10.35	35	-	2.06	1.79	2.13	1.97	2.48	2.21	1.17
25	Kansai	T2	OEC	17.00	16.00	-	-	1.04	1.02	1.59	1.02	1.60	1.25	1.29
26	SintKatelijne	A1	CEC	0.975	0.855	10	(0.2)	2.02	1.70	1.40	1.96	1.12	1.28	1.19
27	SintKatelijne	A4	CEC	1.66	1.41	8	(0.2)	1.81	1.59	1.54	1.76	1.27	1.43	1.33
28	Sandpoint	p	CEC	1.915	1.85	12	(0.2)	0.72	0.81	1.23	0.83	0.95	0.84	1.41
29	WestDelta	LS1	OET	4.29	3.95	24	-	0.98	1.08	0.91	0.97	0.96	1.18	0.81
30	Onsoy2	O1-1	OET	0.519	0.519	12	(0.3)	0.98	1.09	0.76	1.18	1.60	1.11	1.29
31	Cowden2	C2-1	OET	1.02	1.02	26	2	1.54	1.30	1.04	1.58	1.30	1.23	1.02

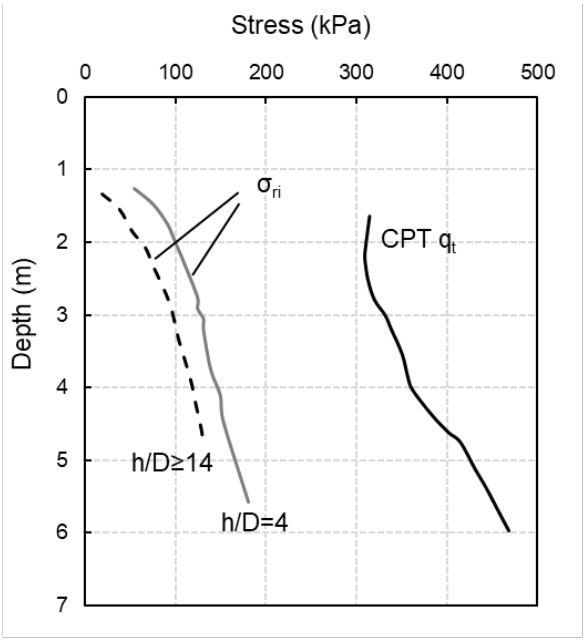
Table 4. Measured and calculated capacities in Unified database (continued)

								Q_m/Q_c						
N	**Site**	**Test**	**Type**	**Q_m (MN)**	**$Q_{m,0.1D}$ (MN)**	**s_{max} (mm)**	**$\dot{s}$ (mm/min)**	**API-11**	**Fugro-96**	**ICP-05**	**NGI-05**	**UWA-13**	**Fugro-10**	**Eqn. 17**
32	Femern	F2-1	OET	3.12	2.42	15	(0.5)	1.81	1.57	2.95	1.62	1.61	1.43	1.31
33	Stjordal	S2-1	OET	0.64	0.64	30	(0.5)	0.59	0.66	0.48	1.31	1.06	0.66	0.87
34	Merville	D1	OEC	1.165	1.04	6	0.3	1.37	1.15	1.50	1.40	1.30	0.96	0.96
35	Merville2	B1S1	CEC	1.55	1.37	6	0.3	1.59	1.38	1.17	1.56	1.02	1.14	0.79
36	Merville2	B3S1	CET	1.4	1.13	6	0.3	1.88	1.56	1.49	1.80	1.23	1.38	0.92
37	Klang	TP1A	OEC	0.635	0.635	20	(0.5)	0.80	0.92	1.06	0.70	1.09	0.82	0.82
38	Riau	G1-T1	OEC	0.425	0.425	30	(0.5)	0.97	1.00	1.64	0.85	1.00	0.84	0.81
39	Riau	G10-T1	OEC	0.5	0.5	30	(0.5)	0.74	0.78	1.17	0.65	0.83	0.70	0.68
40	Riau	G6-T1	OEC	0.7	0.7	30	(0.5)	0.72	0.77	1.20	0.63	0.81	0.67	0.66
41	GoldenEars	SC	CEC	2.8	2.8	20	(0.1)	1.39	1.43	1.86	1.25	1.48	1.35	1.26
42	LuluIsland	UBC1	CEC	0.225	0.225	15	(0.3)	0.58	0.62	0.41	0.68	1.08	0.82	0.83
43	Borsa	P1&2	OET	1.615	1.615	40	1.4	0.48	0.56	0.37	0.85	0.80	0.60	1.38
45	Quebec	9	CET	0.426	0.37	15	(0.2)	0.84	0.80	1.30	0.79	0.89	0.77	0.91
46	Maskinonge	p3	CEC	0.61	0.53	3	0.4	1.37	1.60	1.89	1.27	1.69	1.32	1.48
47	Maskinonge	p4	CEC	0.4	0.4	6	0.4	0.99	1.17	1.38	0.92	1.24	0.96	1.03
48	Maskinonge	p5	CEC	0.88	0.785	17	0.4	0.95	1.18	1.64	0.85	1.22	0.97	1.07
49	Goteborg	a	CEC	0.23	0.23	5	1	0.86	0.91	1.27	0.84	0.99	0.79	1.00

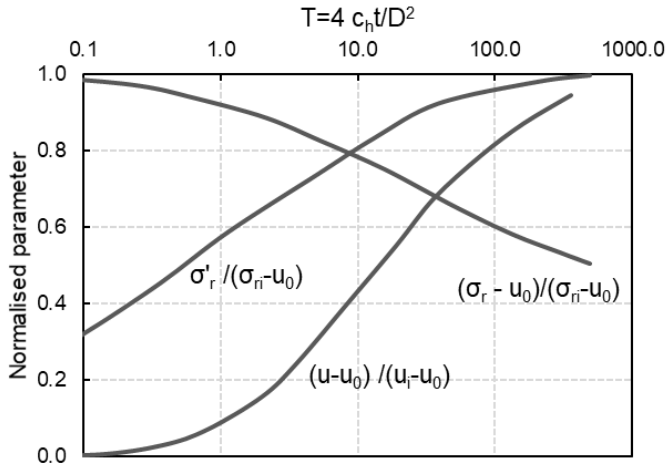
Table 5 Statistics for Q_m/Q_c for Unified database for different τ_f formulations

Method	Correlation type with τ_f	Mean Q_m/Q_c	CoV for Q_m/Q_c	Reference
API	s_u & s_u/σ'_v	1.05	0.43	API (2011)
Fugro-96	s_u, h/D & s_u/σ'_v	1.04	0.35	Kolk & van der Velde (1996)
ICP-05	OCR, σ'_v, h/D*, δ, S_t & σ'_v	1.12	0.55*	Jardine et al. (2005)
NGI-05	s_u, s_u/σ'_v, I_p & σ'_v	1.1	0.36	Karlsrud et al. (2005)
UWA-13	q_t & h/D*	1.12	0.33	Lehane et al. (2013)
Fugro-10	q_{net}, h & q_{net}/σ'_v	0.98	0.37	Van Dijk & Kolk (2010)
Equation 17	q_t , h/D* & S_t	0.99	0.23	This paper

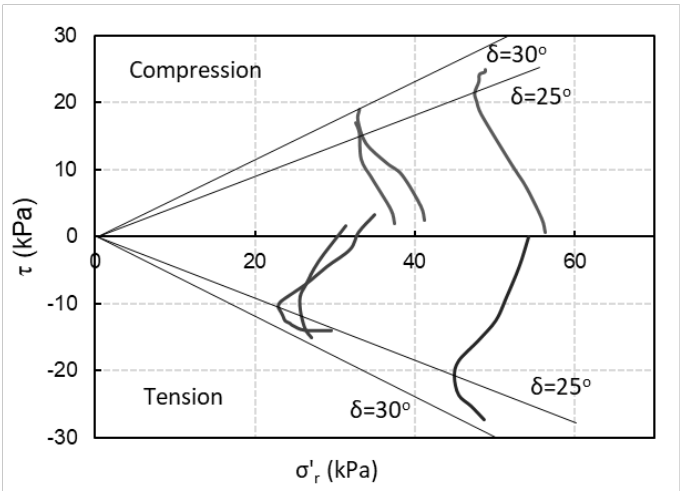
*Note this high CoV arises because of uncertainty related to the parameters required by this approach for many of the database piles



(a)



(b)



(c)

Figure 1 Responses recorded in low OCR clay (a) Radial total stresses during installation (b) Normalised stress changes during equalisation and (c) Shear stress variations with radial effective stress during pile load testing (data from Lehane 1992)

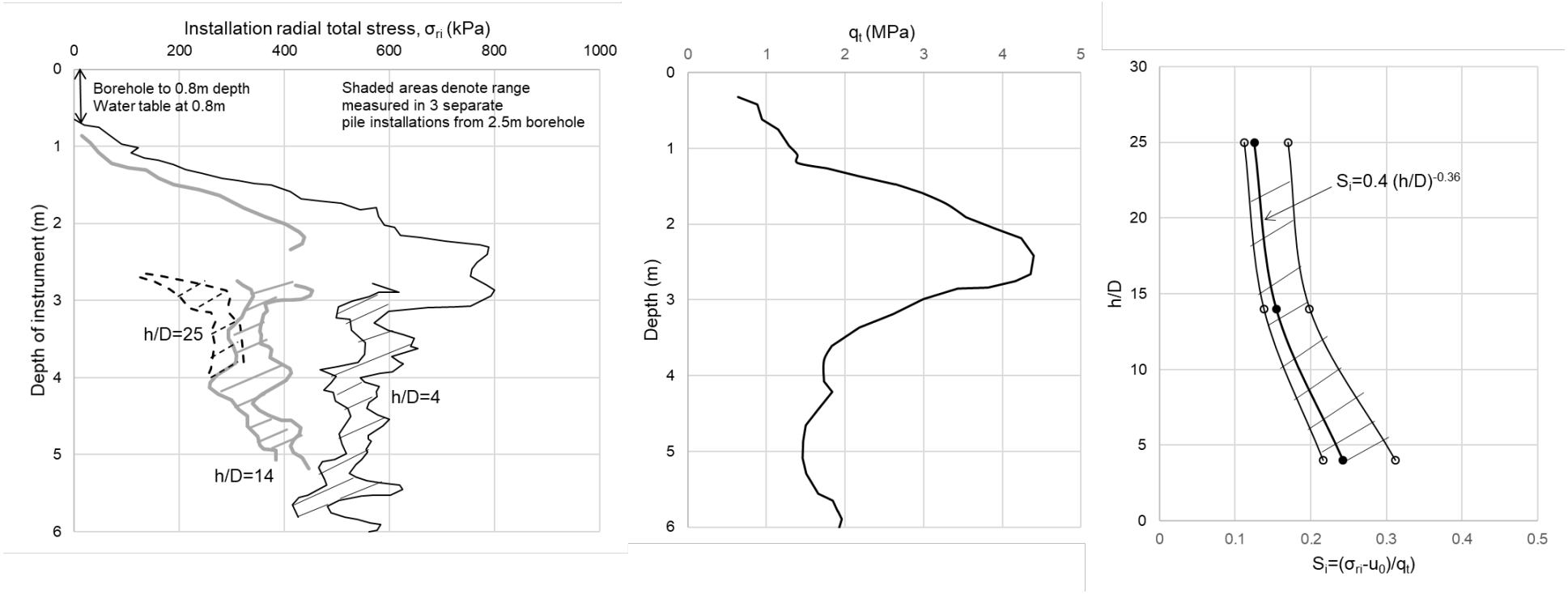
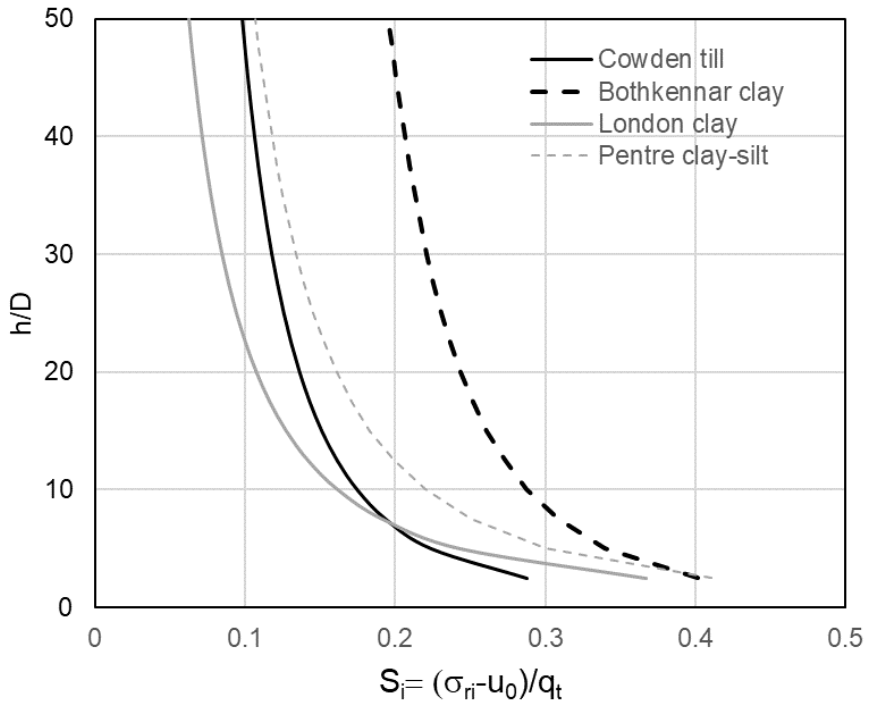
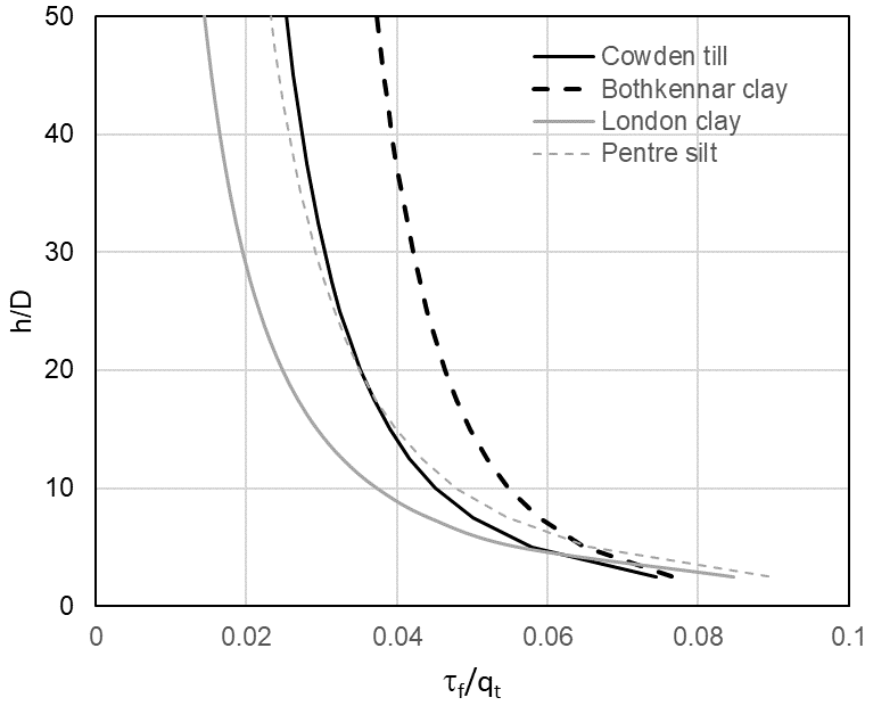


Figure 2. Instrumented pile tests at Cowden (a) Radial stresses recording during installation, (b) CPT resistance profile and (c) Variation of S_i with h/D

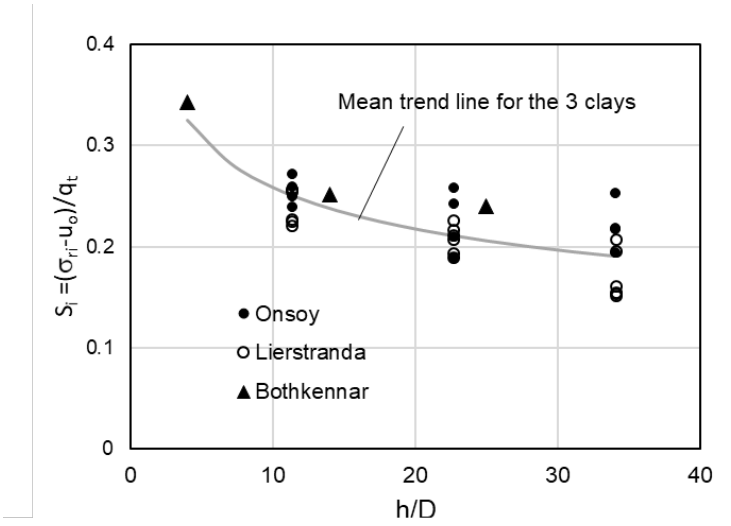


(a)

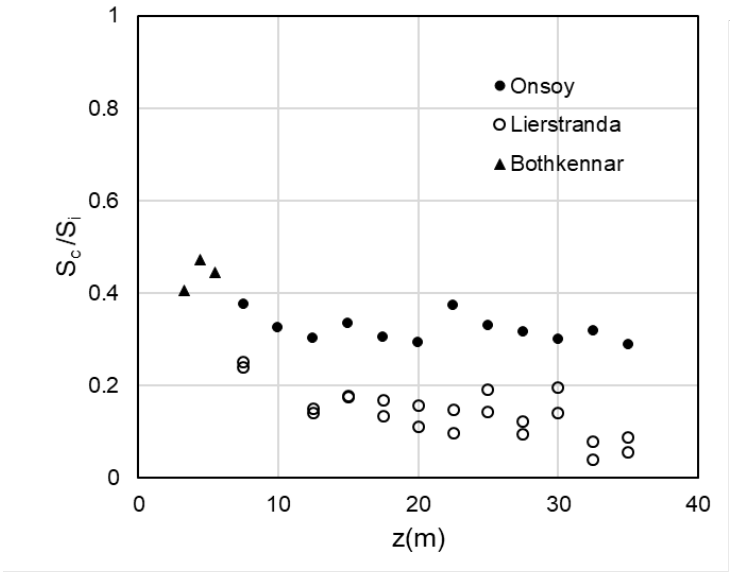


(b)

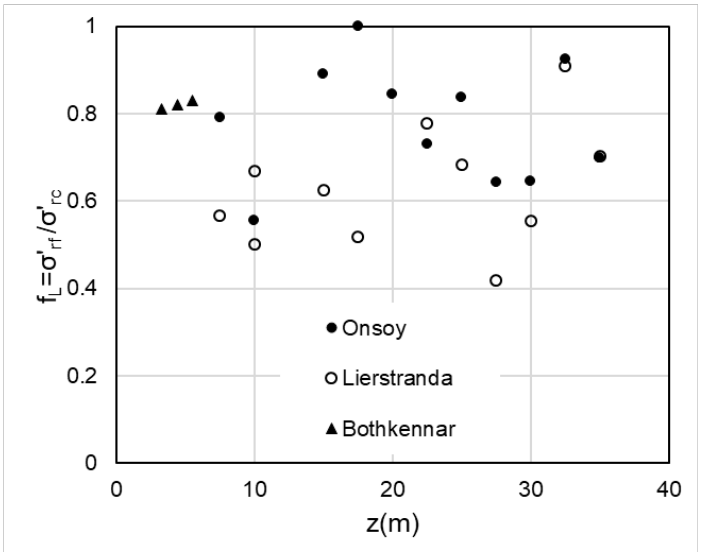
Figure 3. Variation of (a) normalised installation radial stress, S_i and (b) normalised peak friction in 4 different clays (recorded by the Imperial College instrumented pile)



(a)



(b)



(c)

Figure 4 Stress coefficients recorded in Onsøy, Lierstranda and Bothkennar clays (data from NGI 1988a, 1999b and Lehane & Jardine 1994a)

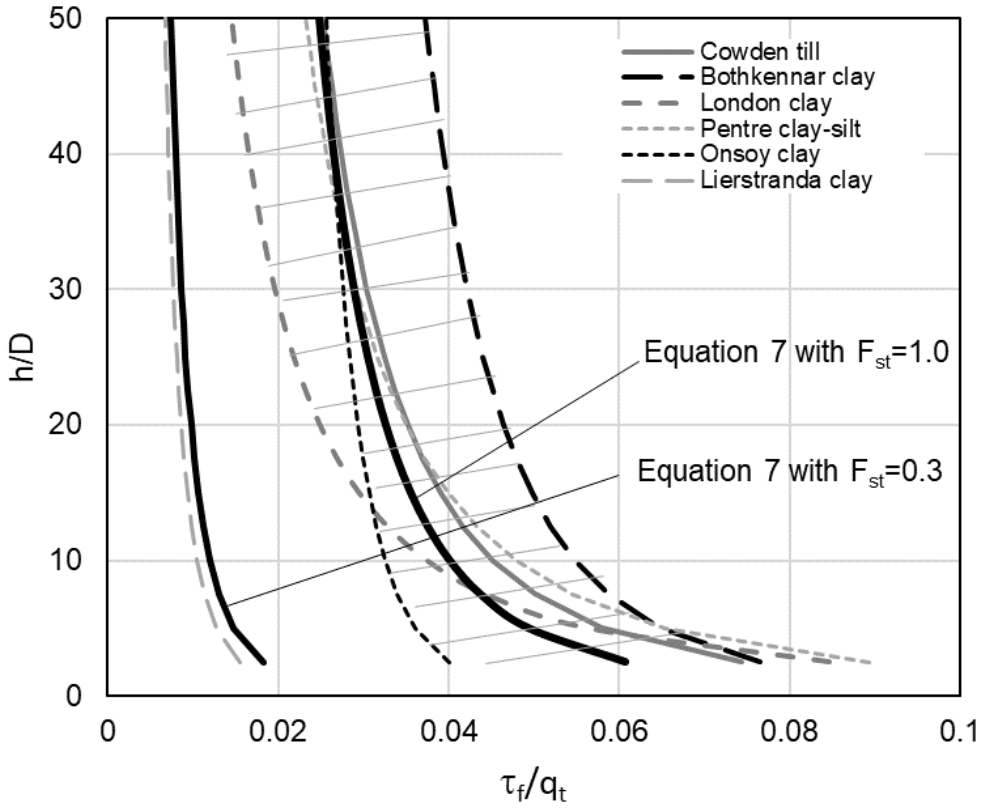
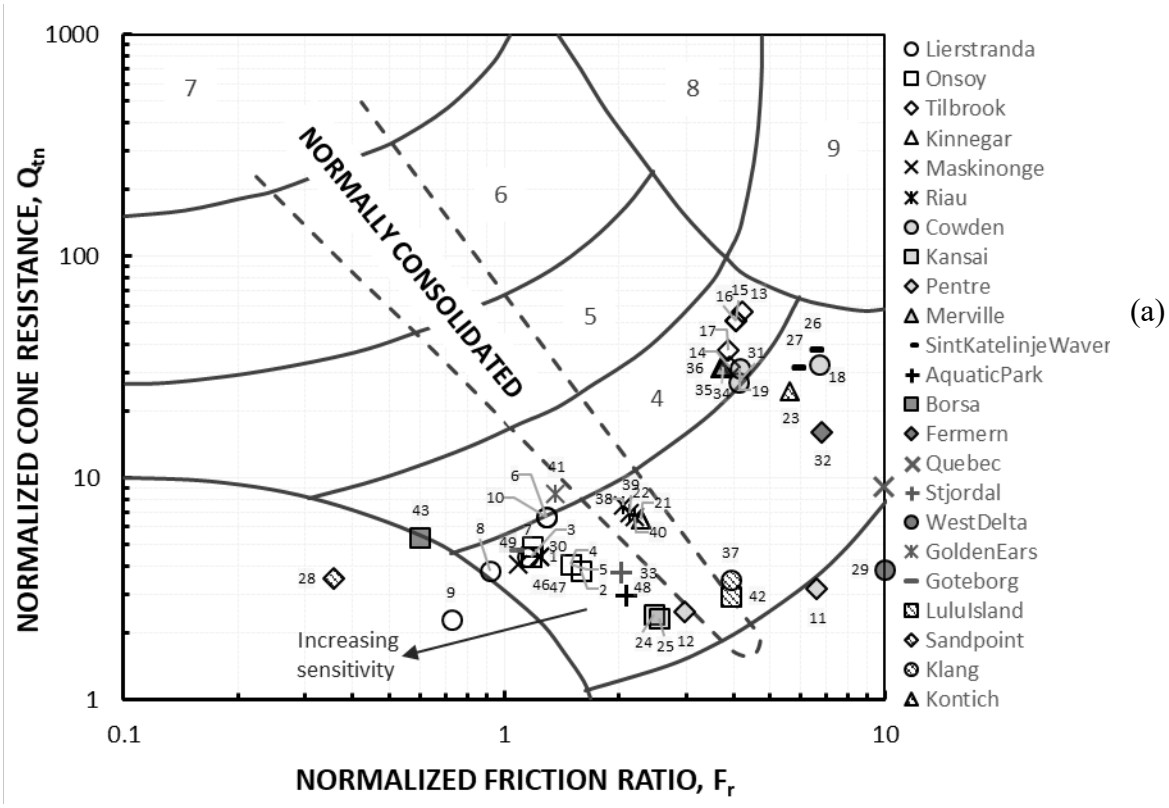
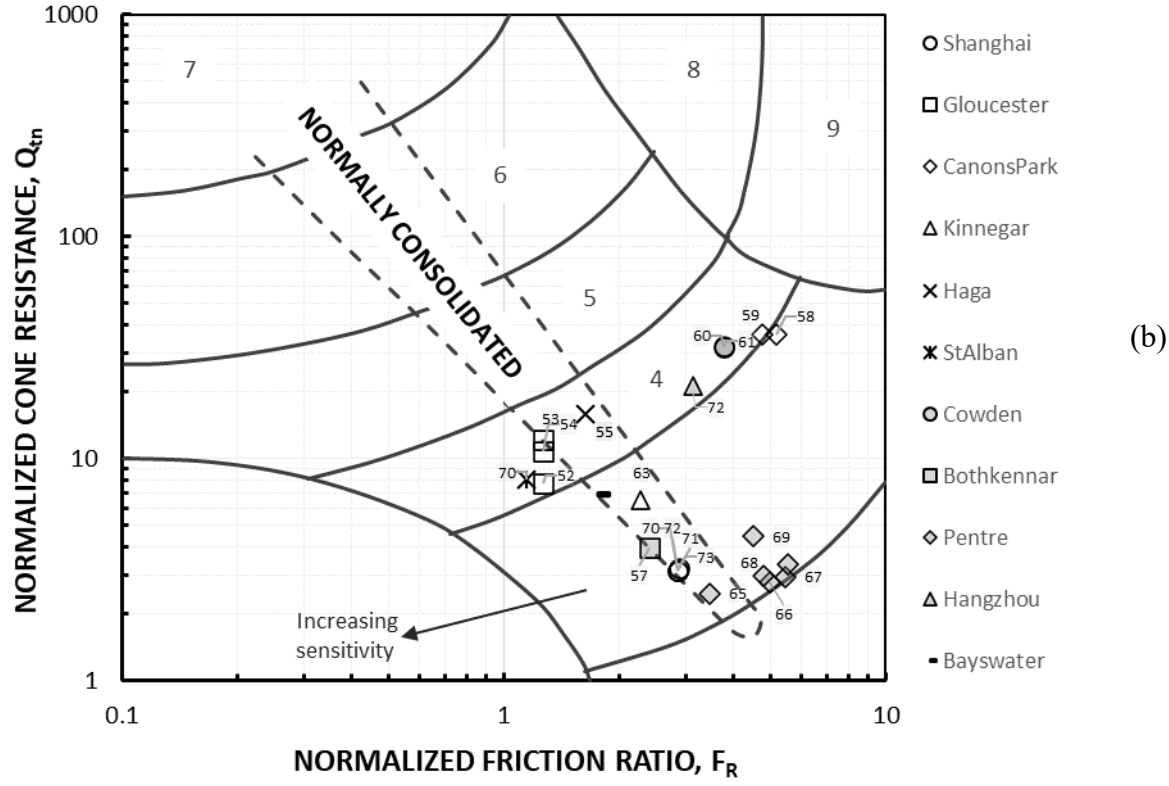


Figure 5. Average variations of τ_f/q_t ratios with h/D inferred from instrumented data in six clays

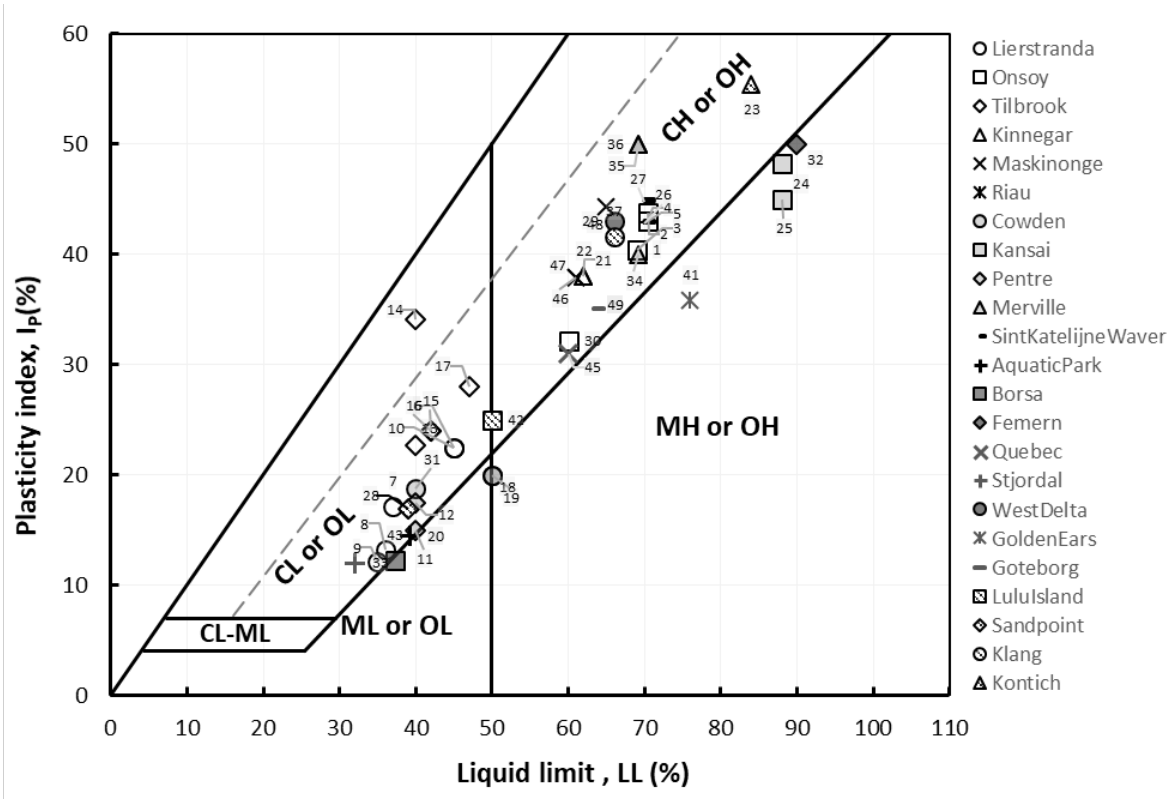


(a)



(b)

Figure 6. Soil behaviour type (SBT) chart using median values at sites of pile tests in the (a) Unified database and (b) Test database. Pile Nos. refer to those in Tables 2 and 3.



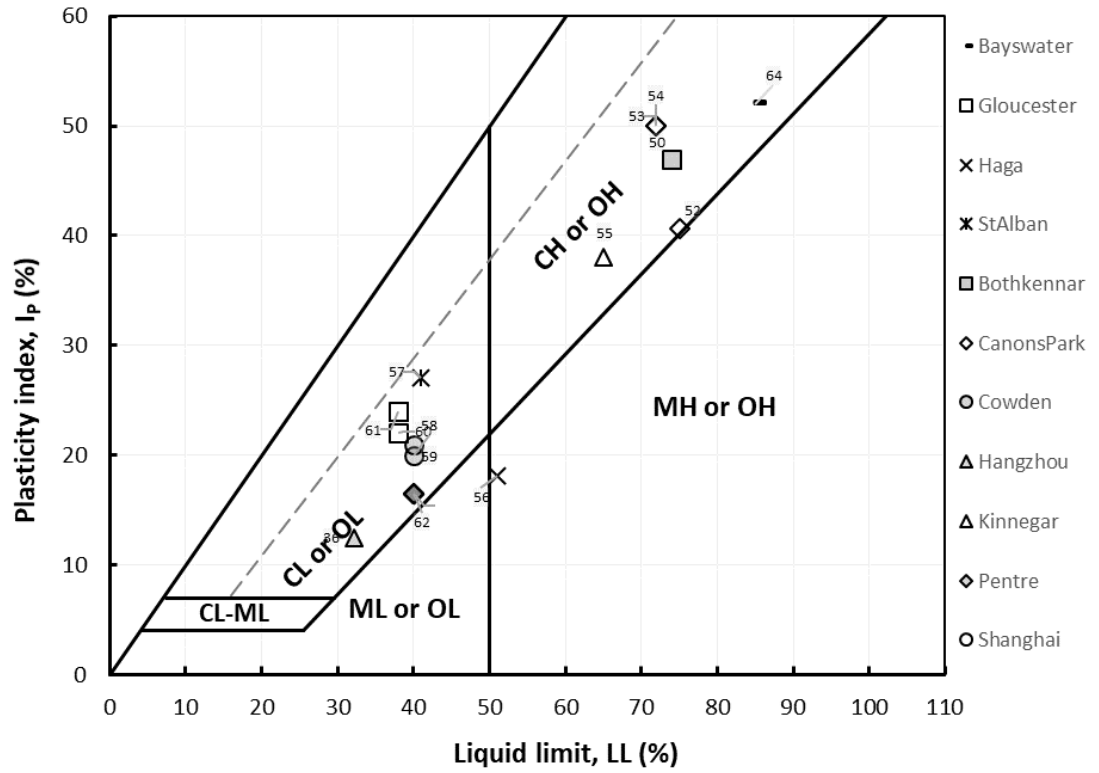


Figure 7. Plasticity chart using median values at sites of pile tests in the (a) Unified database and (b) Test database. Pile Nos. refer to those in Tables 2 and 3.

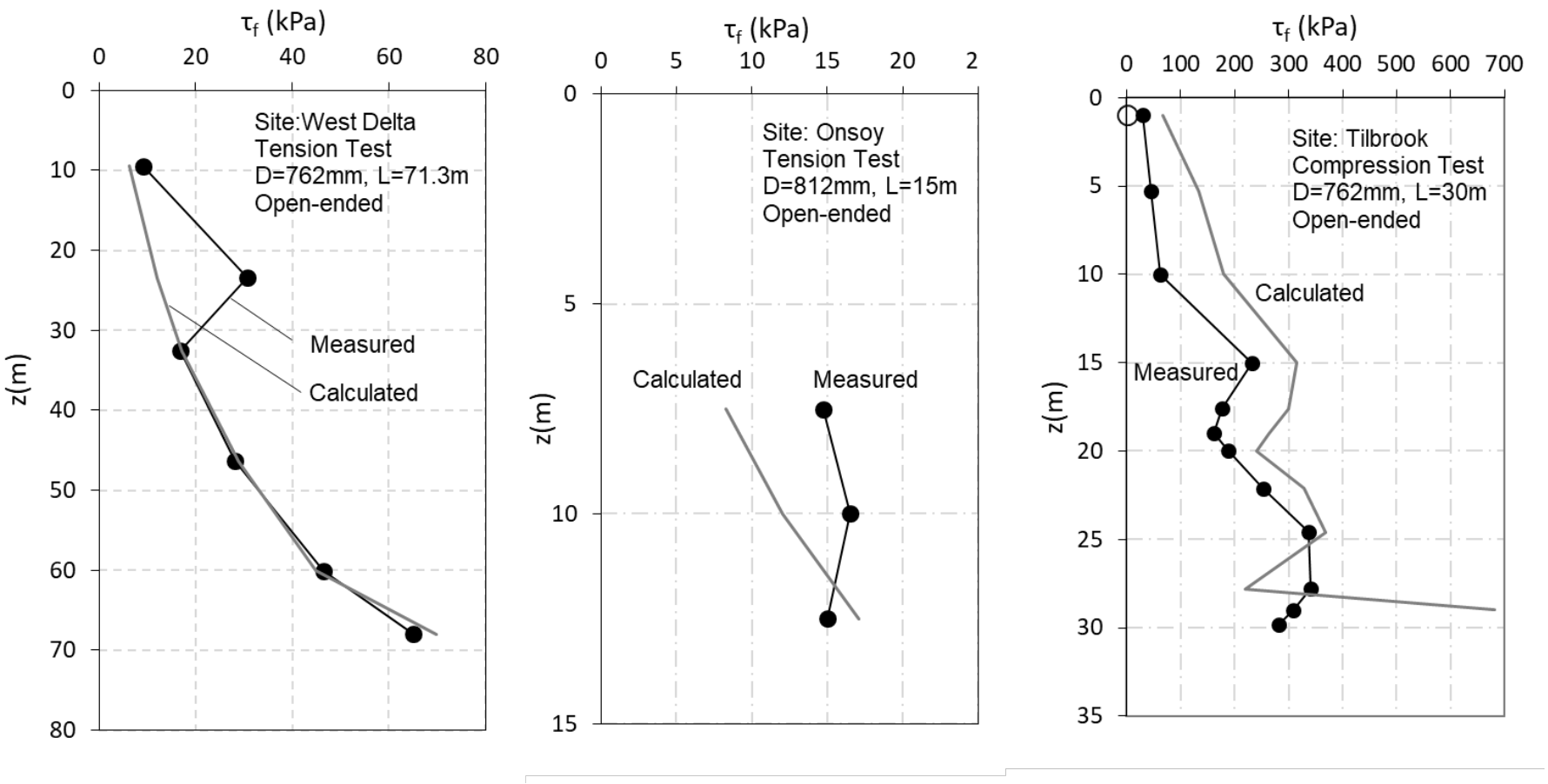


Figure 8. Comparison of measured and calculated ultimate shaft friction profiles for three test piles in the Unified database

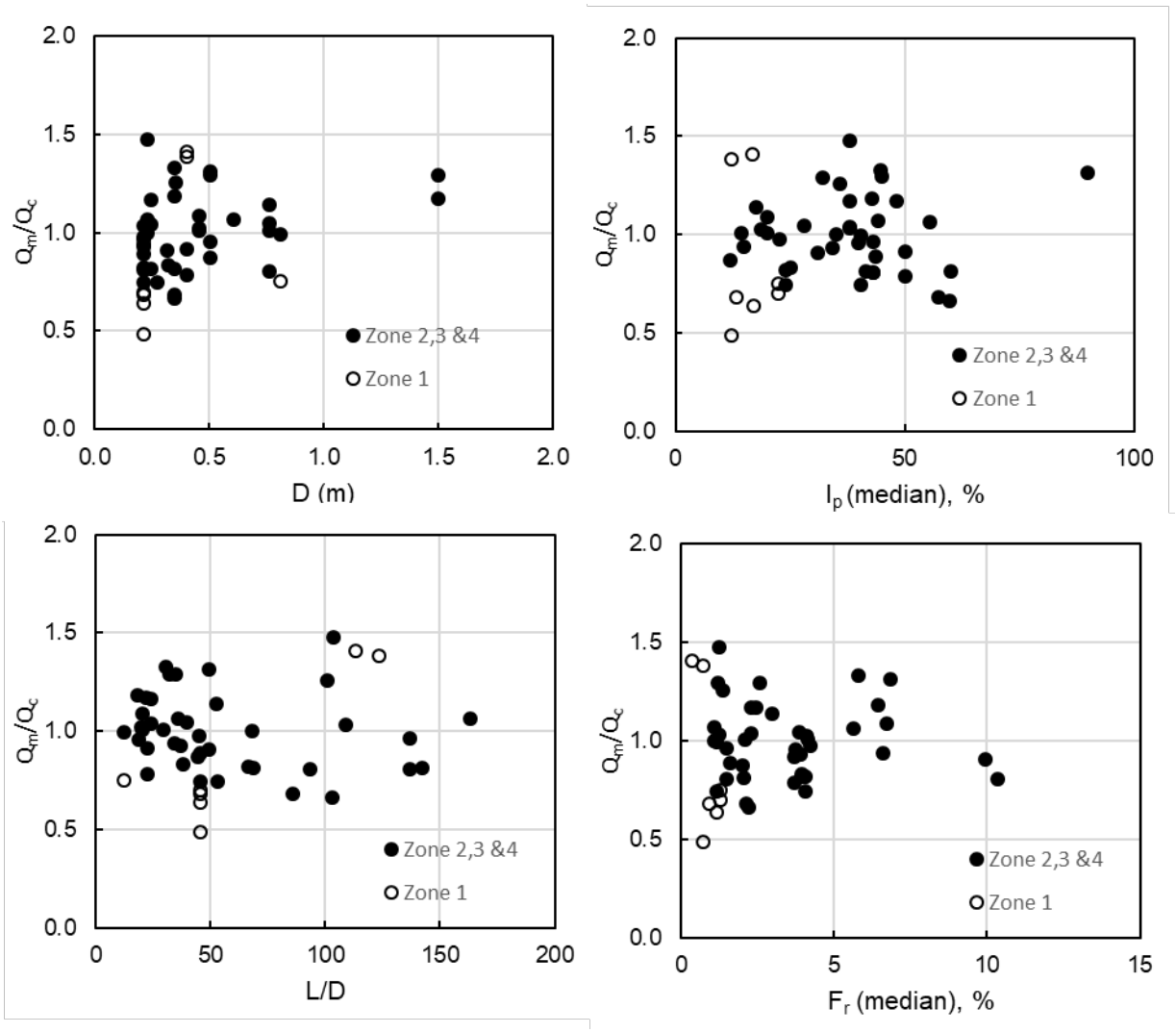


Figure 9. Variations of ratio Q_m/Q_c with D, L/D, I_p and F_r for Unified database (determined using Equation 17)

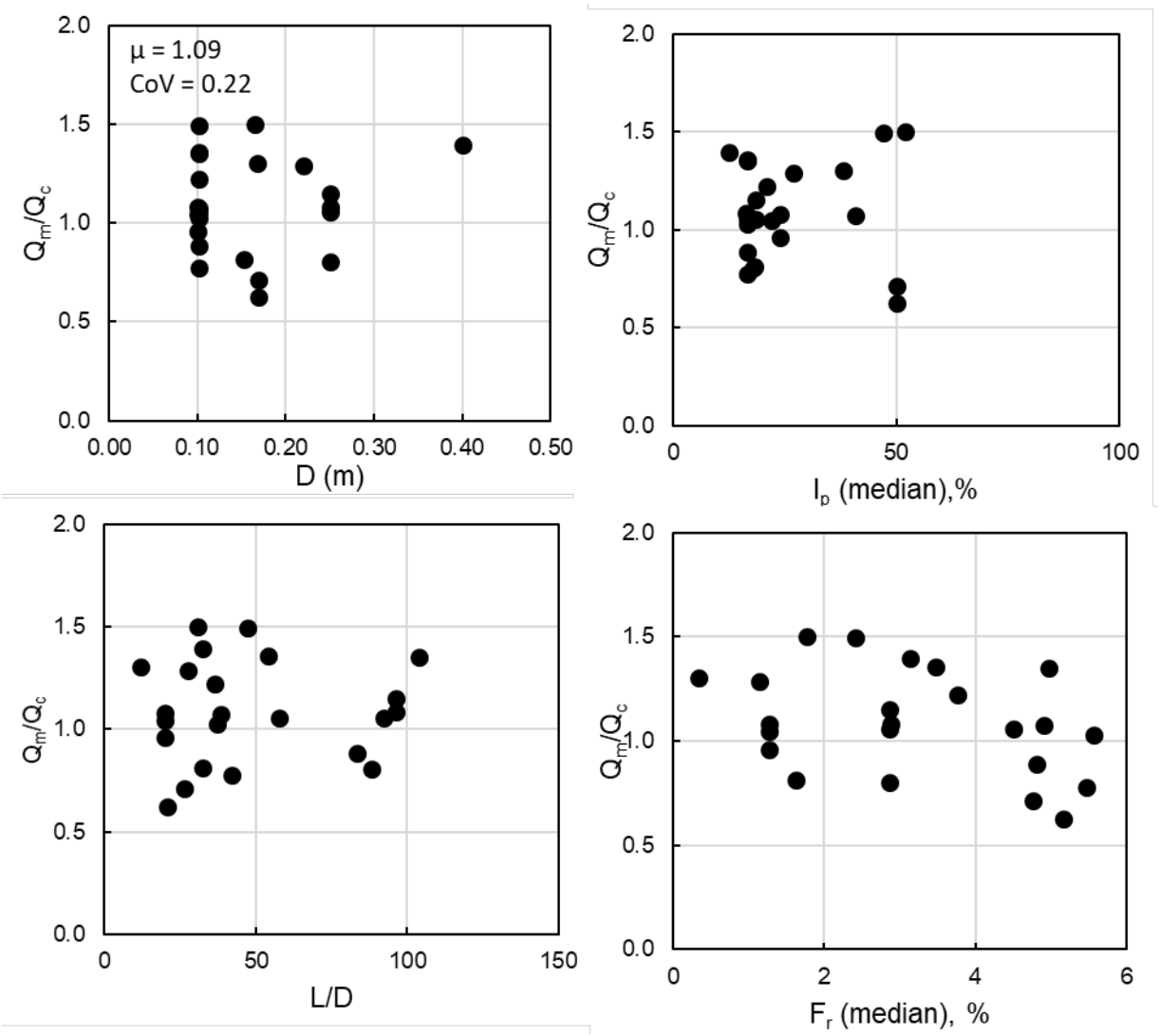


Figure 10. Variations of Q_m/Q_c with D, L/D, I_p and F_r for Test database (determined using Equation 17)